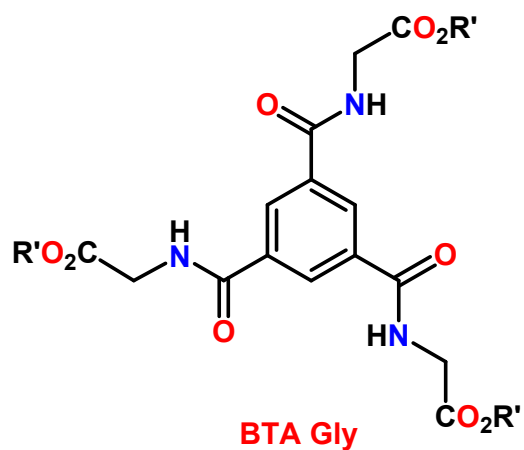


Experimental and computational diagnosis of the fluxional nature of a benzene-1,3,5-tricarboxamide-based hydrogen-bonded dimer

M. Raynal,* Y. Li, C. Troufflard, C. Przybylski, G. Gontard, T. Maistriaux, J. Idé, R. Lazzaroni, L. Bouteiller, and P. Brocorens*

Supporting Information

Chart S1 Chemical structures of the BTA monomers mentioned in this study	2
Supplementary Material (Table S1, Figures S1-S8)	3
Modification of the Dreiding force field (Tables S2-S3, Figures S9-S10)	12
Procedure for the determination of the fraction of HB acceptors in BTA Gly dimers	16
Synthesis of BTA Gly^{t-Bu}	17
¹ H NMR spectrum of BTA Gly^{t-Bu} (acetone -d ₆)	18
¹³ C{ ¹ H} NMR spectrum of BTA Gly^{t-Bu} (acetone -d ₆)	18
Computed infrared spectra (Tables S4-S14, Figure S11)	19
References	31



$R' = \text{H}$, acid BTA, $R' = \text{Me}$, BTA Gly^{Me}
 $R' = t\text{-Bu}$, BTA Gly^{t-Bu} } This
 $R' = \text{C}_{12}\text{H}_{25}$, BTA Gly } work

Chart S1 Chemical structures of the BTA monomers mentioned in this study

Supplementary Material (Table S1, Figures S1-S8)

Table S1 Distances and angles related to hydrogen bonding and aromatic interactions in the X-ray structures of **BTA Gly^{t-Bu}** (spiral-type and dissymmetric dimeric structures), of **acid BTA** (spiral-type dimeric structure) and of **BTA Gly^{Me}** (stacks).

molecule	space group	Distance (Å), angle (°) and coaxiality (Å) ^(a) of BTA rings	amide N-H...O=C distance (Å)	amide N-H...O=C angle (°)	ester N-H...O=C distance (Å)	ester N-H...O=C angle (°)	C-C-C=O ^(c) dihedral angle (°)
BTA Gly^{t-Bu} spiral-type dimer [6 - 6/0]	<i>Pa-3</i>	3.558(2)	none	none	2.174(1)	159.77(8)	19.9(2)
		0					
		0					
acid BTA·3H₂O spiral-type dimer ¹ [6 - 6/0]	<i>R-3</i>	3.660(3)	none	none	2.128(2)	159.1(3)	21.5(3)
		0					
		0					
BTA Gly^{t-Bu} dissymmetric dimer [4 ₂ - 2/2]	<i>P2₁/c</i>	3.471(3)	2.168(2) ^(b) <i>intra</i>	140.62(12) ^(b)	2.064(2) <i>intra</i>	161.45(13)	23.1(3), 36.0(3) 40.7(3), 27.0(3) 21.7(3), 14.8(3)
		6.25(8)	2.140(2) <i>intra</i>	146.32(12)	2.264(2) <i>intra</i>	147.83(12)	
		0.5	2.026(2) <i>inter</i>	171.76(11)	2.455(2) <i>Harom.</i>	146.13(12)	
			2.027(2) <i>inter</i>	167.47(12)	2.472(2) ^(b) <i>C5-ring</i>	98.17(12) ^(b)	
BTA Gly^{Me}·0.5 H₂O stacks ²	<i>P2₁/n</i>	3.503(2)	1.961(3)	161.54(22)	none	none	36.39(22)
		1.54(6)	2.007(3)	167.20(21)			35.95(22)
		0.3	2.097(3)	164.48(20)			43.70(22)

(a) Coaxiality corresponds to the distance between the centroid of one BTA ring and the point corresponding to the orthogonal projection of the other centroid.

(b) The N-H proton is bifurcated.

(c) Dihedral angle between the aromatic core and the amide groups.

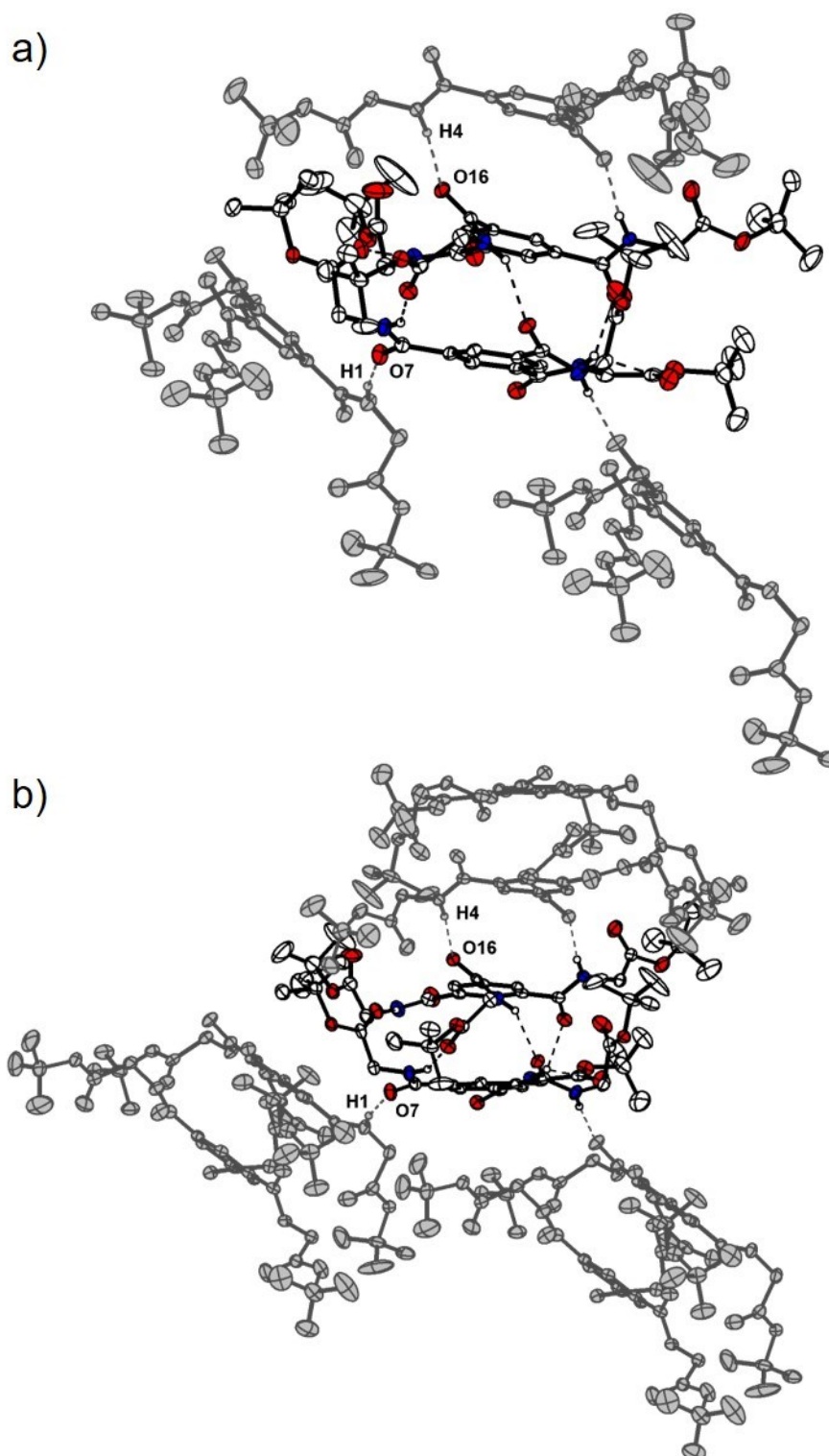


Figure S1 Representation of the molecules engaged in hydrogen bonding interactions with a dissymmetric dimer in the X-ray structure of **BTA Gly^{t-Bu}**. (a) ORTEP representation of the dissymmetric dimer (in colour) and the three interacting molecules (in grey). (b) ORTEP representation of the dissymmetric dimer (in colour) and the surrounded dimers (in grey). Intermolecular hydrogen bonds occur through amide functions exclusively.

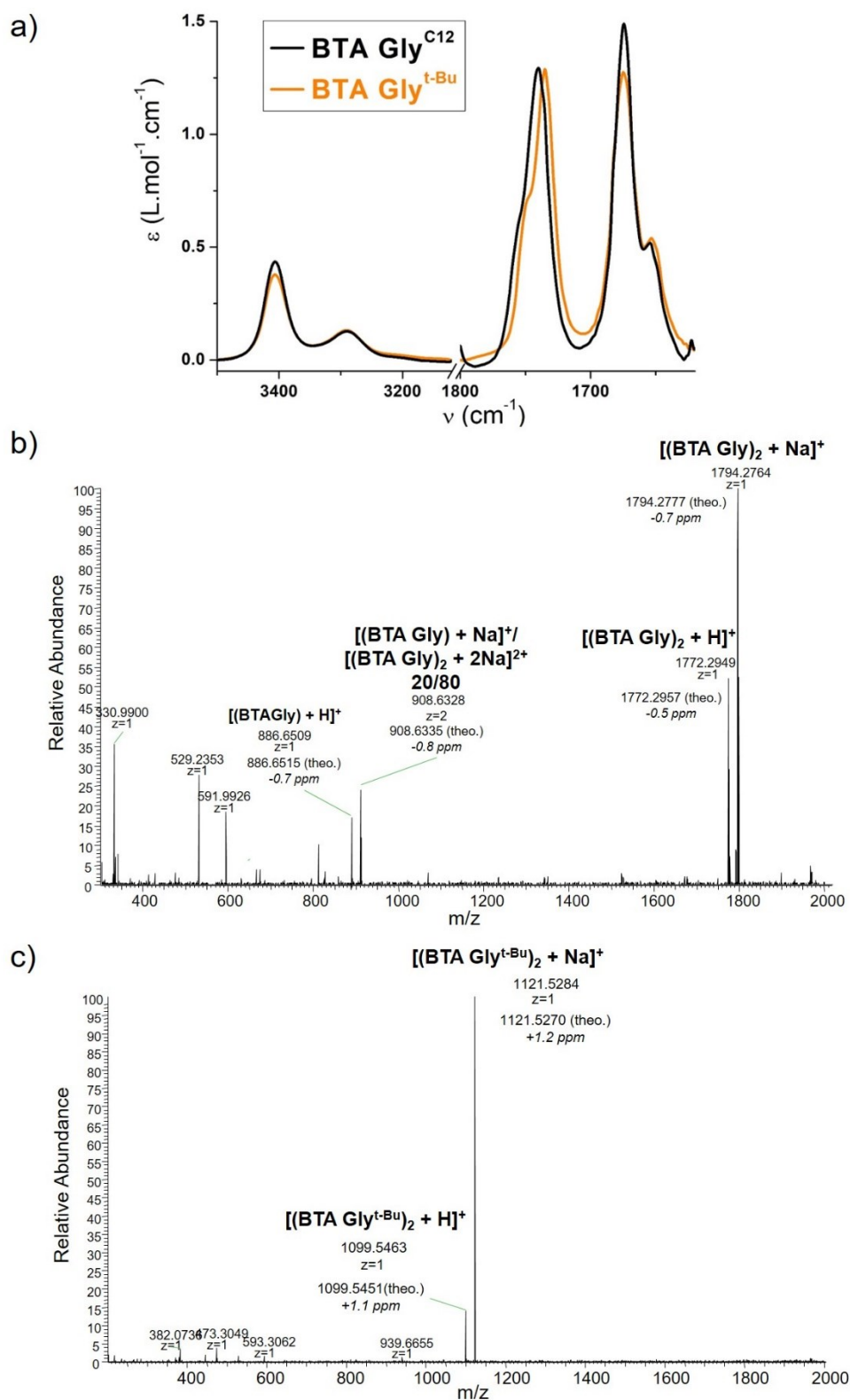


Figure S2 (a) FT-IR analyses of **BTA Gly** and **BTA Gly^{t-Bu}** in toluene (5 mM, 293 K). Zoom of the N–H and the C=O regions (ester and amide I). (b) ESI-HRMS analysis of **BTA Gly**. (c) ESI-HRMS analysis of **BTA Gly^{t-Bu}**.

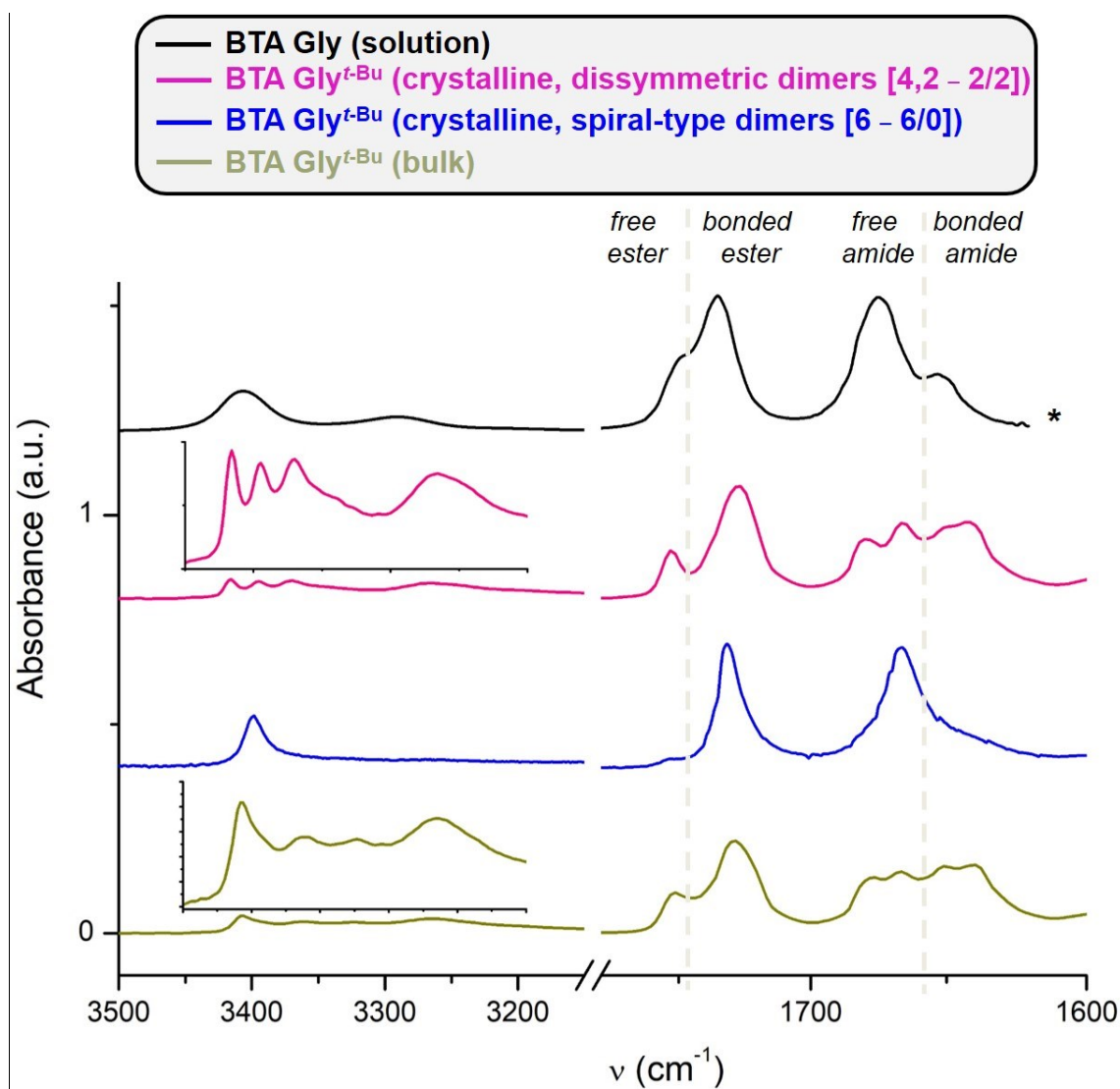


Figure S3 Comparison of the FT-IR spectra of **BTA Gly^{t-Bu}** (bulk and single crystals) and **BTA Gly** (5 mM toluene solution). Zoom on the N–H, ester carbonyl, and amide I regions. The solids of **BTA Gly^{t-Bu}** were obtained after evaporation of a DCM/AcOEt solution (bulk) or after crystallisation in DCM/hexane (single crystals). The two types of single crystals correspond to spiral-type dimers and dissymmetric dimers, respectively; they were separated based on their shape. Nevertheless, single crystals of the dissymmetric dimers are contaminated with single crystals of spiral-type dimers. The spectra are shown with an offset of 0.4 Abs. * indicates that absorbance saturates in this region of the FT-IR spectrum.

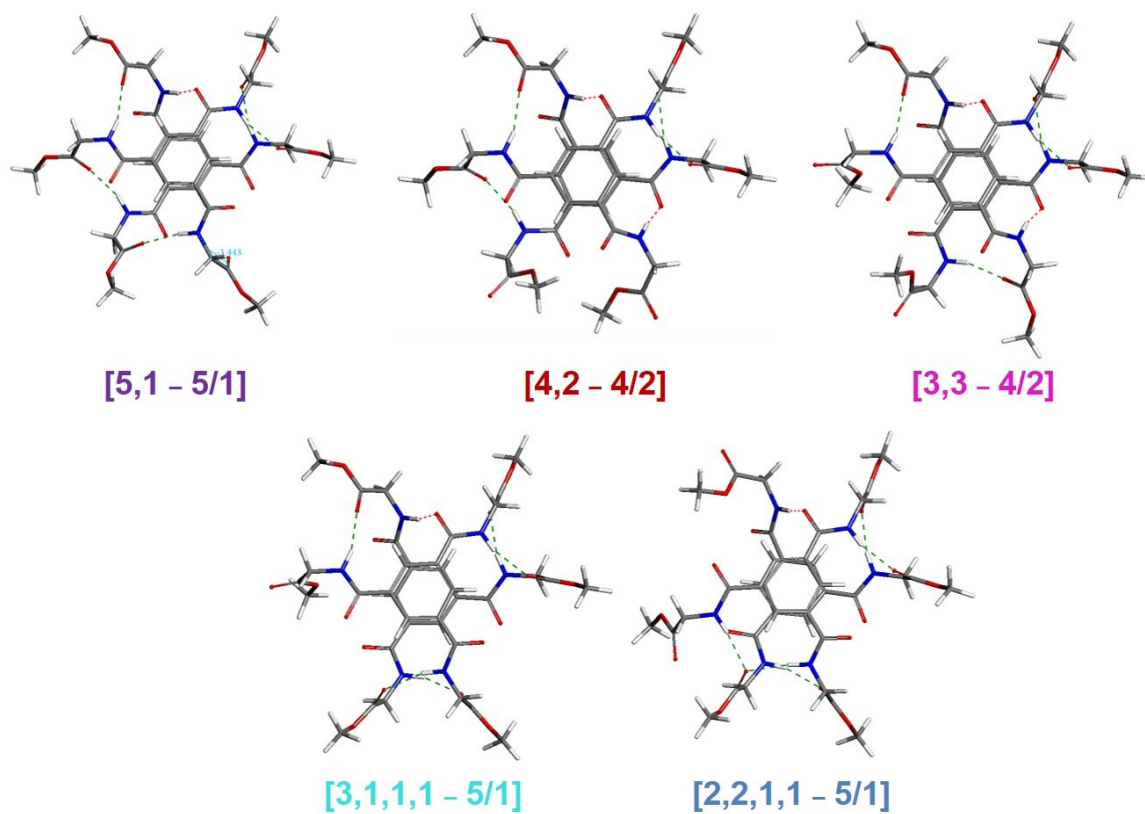


Figure S4 Conformations of BTA Gly^{Me} dimers, belonging to [5,1], [4,2], [3,3], [3,1,1,1] and [2,2,1,1] families, optimized at the B3LYP-GD3BJ/cc-pVDZ level.

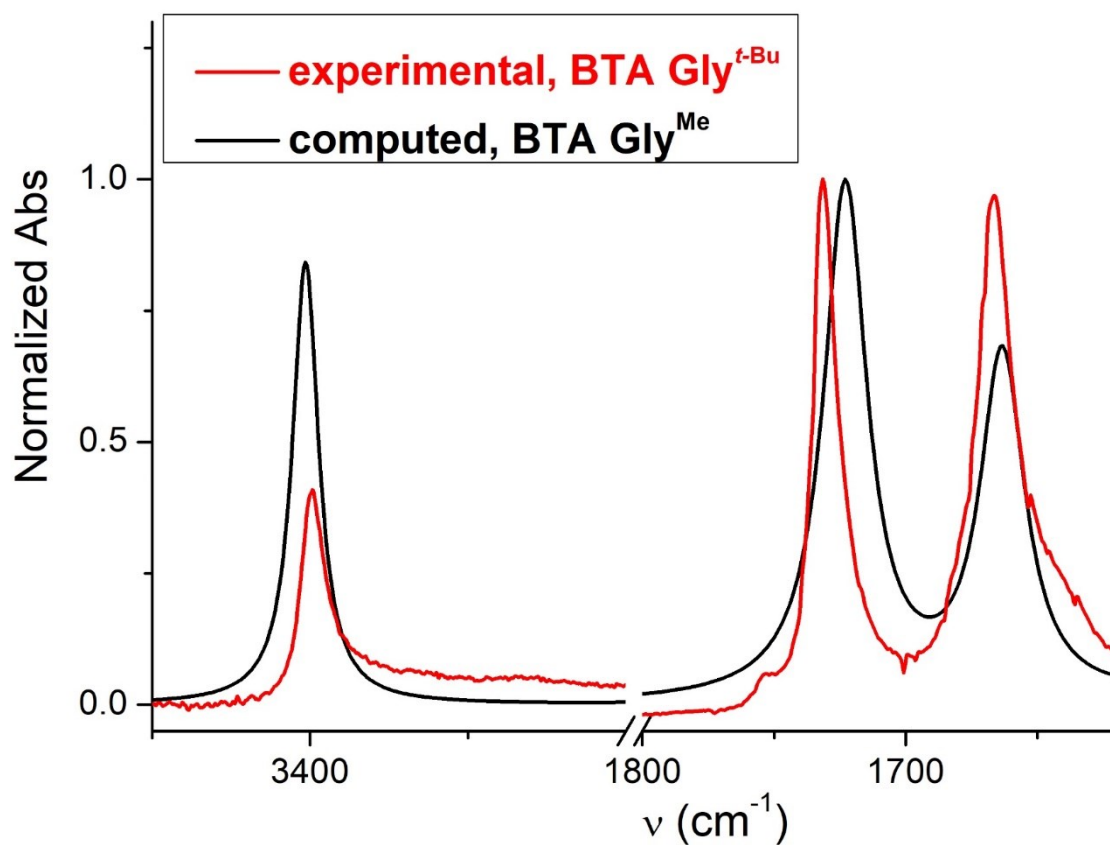


Figure S5 Computed (for **BTA Gly^{Me}**) and experimental (for **BTA Gly^{t-Bu}**, single crystals) FT-IR spectra of the spiral-type dimers [6 - 6/0]. Zoom on the N-H, ester carbonyl, and amide I regions. The spectra have been normalized to the maximum of the band corresponding to the ester carbonyl vibration.

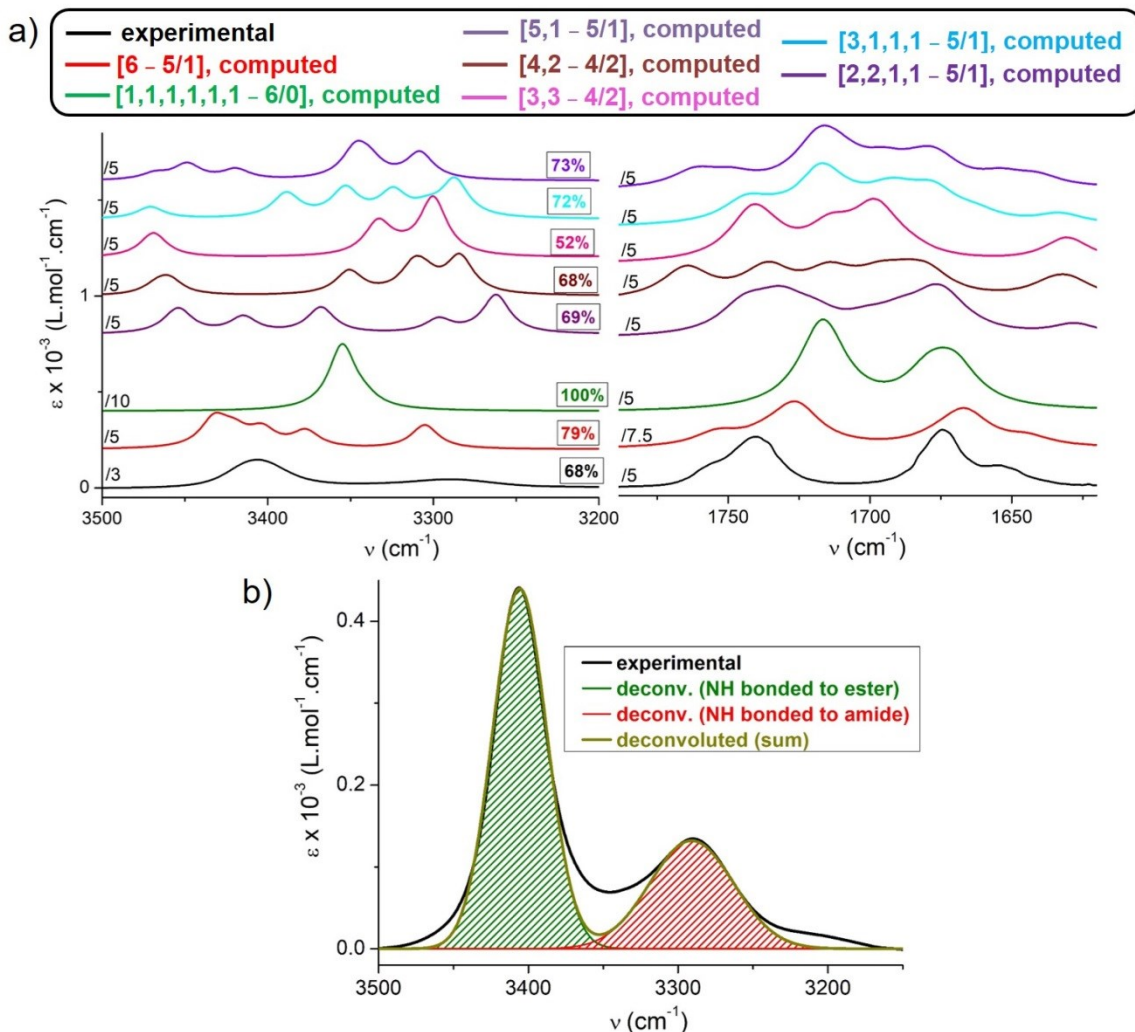


Figure S6 a) Experimental (**BTA Gly**) and computed (**BTA Gly^{Me}**) FT-IR spectra for the conformations that are not included in Figure 5. The intensity of certain spectra has been decreased as indicated in order to allow an easier comparison of the experimental and computed FT-IR bands. The computed spectrum of the conformation [6 - 5/1] is shown because of its similarity with the experimental one. The percentages correspond, for each spectrum, to the fraction (in area %) of the band(s) corresponding to N–H bonded to ester carbonyls such as $f = \text{area of the band(s) corresponding to N–H bonded to ester carbonyls} / \text{sum of the areas of the bands corresponding to N–H}$. These areas have been extracted from the respective deconvoluted spectra. b) Deconvolution of the experimental FT-IR spectrum of **BTA Gly** in order to determine the contribution of N–H bonded to ester and N–H bonded to amide in the N-H region.

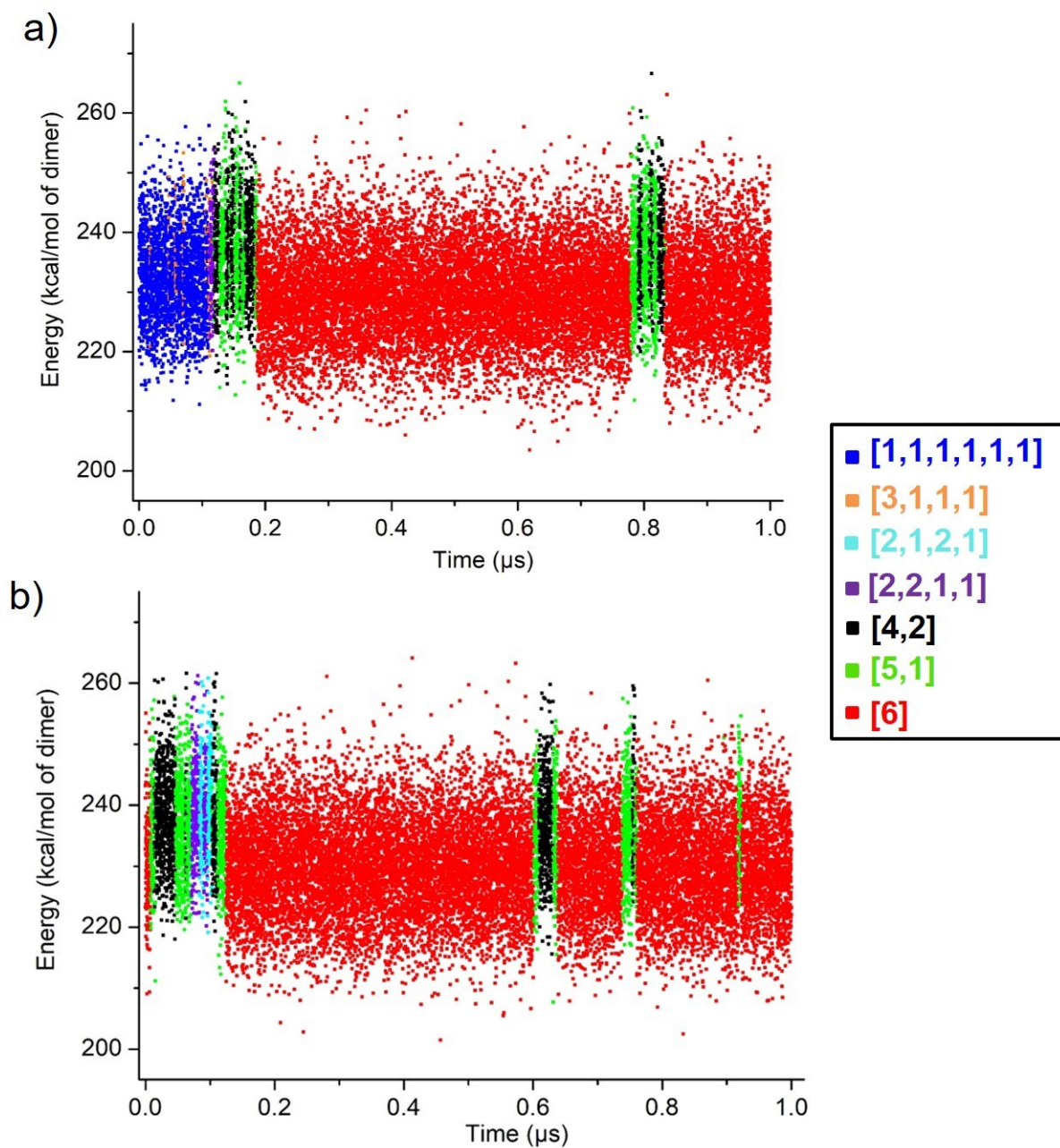


Figure S7 Comparison of the MD trajectories of a **BTA Gly^{Me}** dimer of the type [1,1,1,1,1,1 - 6/0] (a) or [6 - 6/0] (b) as starting conformations.

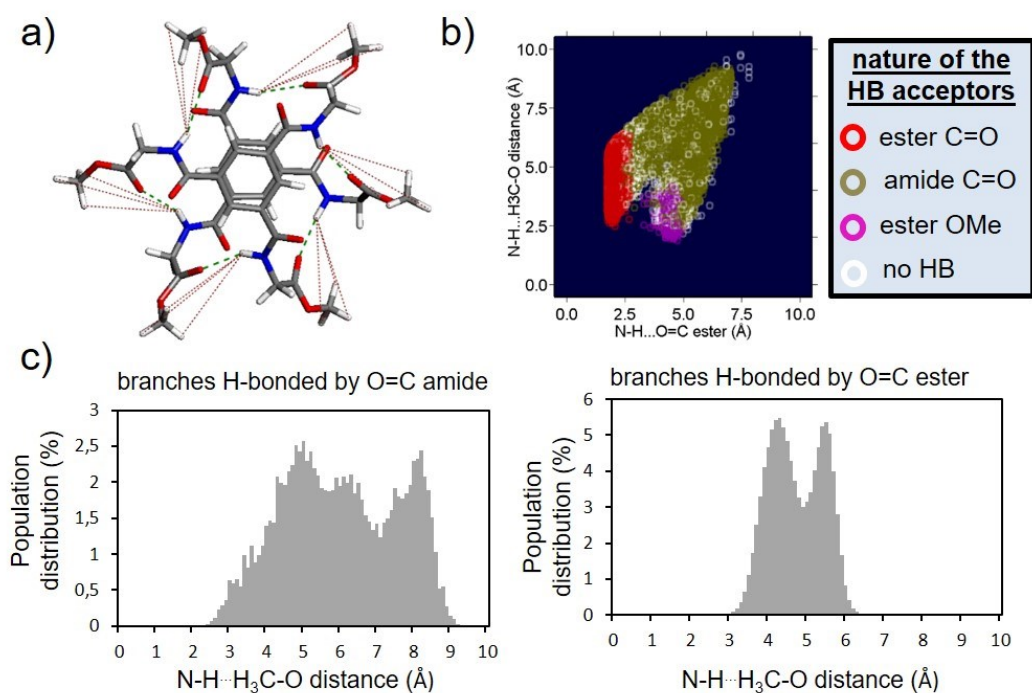
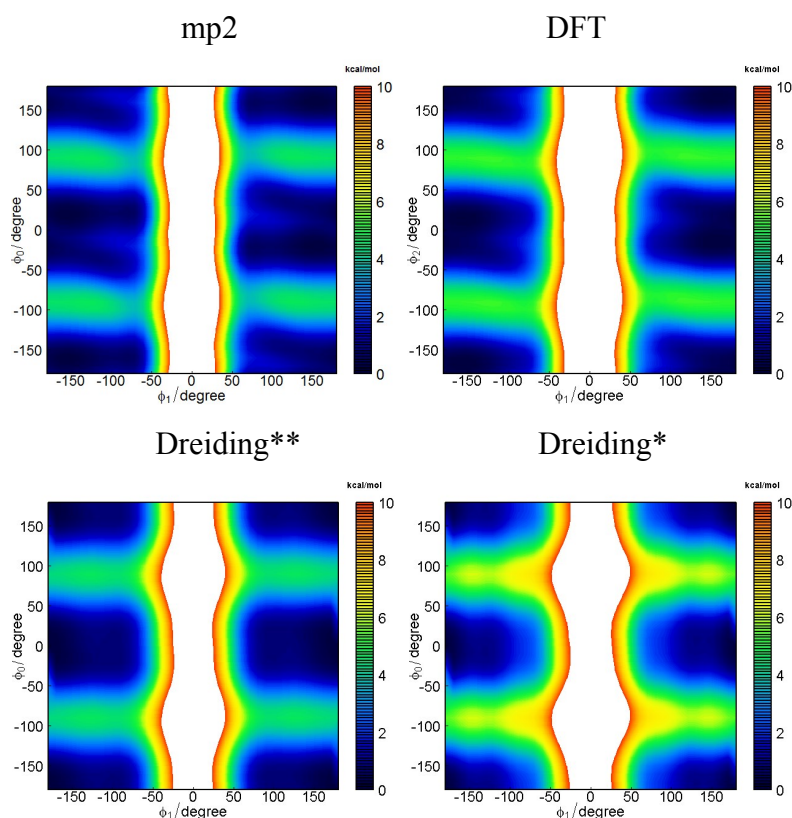
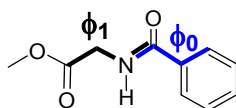


Figure S8 a) Measurements of selected N-H...H₃C-O distances and N-H...O=C ester distances on a [6 - 6/0] conformer of **BTA Gly^{Me}**. b) Plot of these distances recorded during the 1 μ s-long MD simulations (Figure 7a) for the spiral [6] conformers. c) Population distribution of the N-H...H₃C-O distances recorded as in (a) during the 1 μ s-long MD simulations for branches of the spiral [6] conformers H-bonded by amide and ester, respectively, as HB acceptors.

Modification of the Dreiding force field (Tables S2-S3, Figures S9-S10)

The Dreiding force field was modified to properly reproduce van der Waals interactions with hydrogen atoms of atom type H₋ (R_0 reduced from 3.195 Å to 2.83 Å).³ The name of this force field is Dreiding*. As the rotational barriers are critical for the molecular flexibility, we also checked that they are correctly reproduced in BTA. For that purpose, we built the Φ_0 - Φ_1 and Φ_1 - Φ_2 energy maps with Dreiding*: a benzene monocarboxamide molecule representative of the BTA region affected by the torsions was considered (see Figure S9), the defined torsions were varied stepwise by 10°, and at each step the geometry was relaxed by MM with the exception of the defined torsions. These energy maps were then compared to reference energy maps similarly obtained with the mp2/cc-pVDZ method, and with the B3LYP-GD3BJ/cc-pVDZ method used to simulate dimers and their IR spectra. The mp2 and DFT energy maps are similar, and differ significantly from those of Dreiding*. Hence, some torsional parameters were adapted or added to have the force field energy maps fitting the mp2 energy maps (Figure S9). The new force field is called Dreiding** and its modified parameters are presented in Table S2.

Φ_0 - Φ_1 energy maps



Φ_1 - Φ_2 energy maps

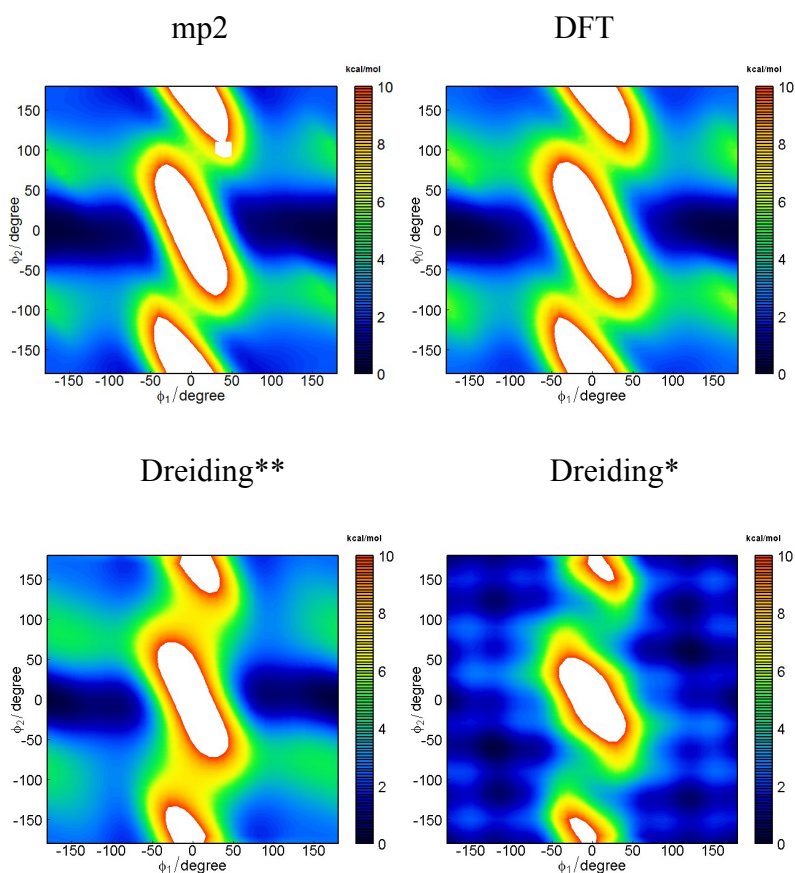
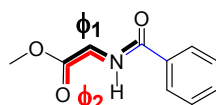


Figure S9 Φ_0 - Φ_1 and Φ_1 - Φ_2 energy maps of the BTA branches obtained by the mp2 quantum chemistry method, and the Dreiding** and Dreiding* force fields. Structure of the molecules used to model the region of BTA affected by the selected torsions.

Table S2 Parameters of torsion types that were modified or added in the Dreiding** force field.

Affected torsion	Atom types	B1 (kcal/mol) d1 n1	B2 (kcal/mol) d2 n2
Φ_2	O_R C_R C_3 H_	0.5 -1 4	1.2 -1 3
Φ_2	O_2 C_R C_3 H_	0.5 -1 4	1.2 1 3
Φ_2	O_R C_R C_3 N_R	8 1 2	5 -1 1
Φ_2	O_2 C_R C_3 N_R	8 1 2	4.7 1 1
Φ_0	O_2 C_R C_R X	22 1 2	
Φ_0	N_R C_R C_R X	22 1 2	

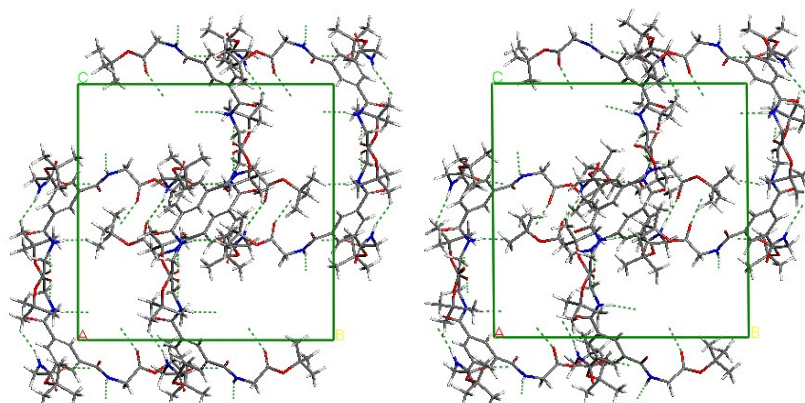
$\Phi 1$	C_R N_R C_3 H_	0.75 -1 3	
$\Phi 1$	C_R N_R C_3 C_R	3 -1 2	
$\Phi 1$	H_A N_R C_3 H_	2 -1 3	
$\Phi 1$	H_A N_R C_3 C_R	3 -1 2	

To further validate Dreiding**, we performed MD simulations of the two experimental crystalline structures of **BTA Gly^{t-Bu}** discussed in the paper. We applied the same simulation parameters as for the dimers, with the exception of the adjustments necessary to deal with the periodicity of the systems: periodic conditions were applied in the NPT ensemble (298K, 10⁵ Pa), the long-range interactions were treated with the Ewald summation method (accuracy of 0.001 kcal/mol), and the Parrinello barostat (cell time constant of 1 ps) was used, which allows all cell parameters to fluctuate during the dynamics. There were no constraints applied. The dynamics were performed during 10 ns. This time scale is long enough to observe any potential competition between amide and ester as hydrogen bond acceptors, as observed in the MD simulations of dimers. The simulations show that the cell parameters are well reproduced (see Table S3), with maximal errors of 1.3% for the spiral structure (*a* and *b* being the most affected parameters), and 2.1 % for the dissymmetric structure (*a* being the most affected parameter); the organization of the molecules and the network of hydrogen bonds (see Figure S10) are also maintained throughout the dynamics, thus showing no competition between amides and esters for hydrogen bonding. These observations support our view that Dreiding** is appropriate to model the **BTA Gly** derivatives.

Table S3 Cell parameters of the spiral and dissymmetric crystal cells of **BTA Gly^{t-Bu}**. The experimental data are compared to averages calculated on 201 structures generated during the 10 ns MD simulation (with the standard deviation indicated).

		a (Å)	b (Å)	c (Å)	α (°)	β (°)	γ (°)
Spiral	Exp.	18.2873(3)	18.2873(3)	18.2873(3)	90.0	90.0	90.0
	Sim.	18.52 ± 0.16	18.52 ± 0.17	18.48 ± 0.17	90.0 ± 1.3	90.0 ± 1.3	90.0 ± 1.3
Dissymmetric	Exp.	13.6976(2)	15.5866(3)	28.4803(5)	90.0	91.1670(10)	90.0
	Sim.	13.99 ± 0.12	15.65 ± 0.29	28.75 ± 0.36	89.9 ± 1.0	90.9 ± 1.4	90.0 ± 1.2

Spiral



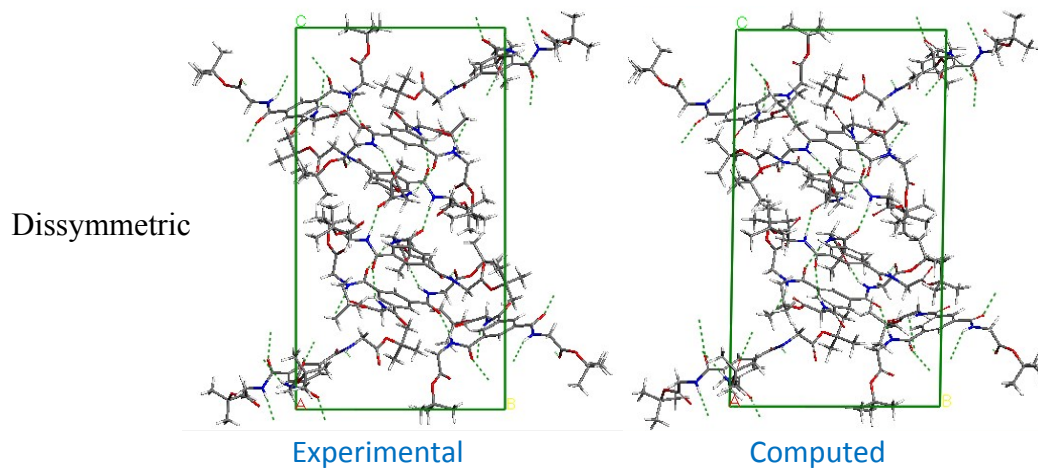


Figure S10 Spiral (top) and dissymmetric (bottom) crystal cells of **BTA Gly^{t-Bu}** observed experimentally (left), and extracted at the end of the 10 ns MD simulation (right).

Procedure for the determination of the fraction of HB acceptors in BTA Gly dimers

The fraction (f , in area %) of the band(s) corresponding to N–H bonded to ester carbonyls such as:

$$f = \frac{\text{area of N - H bonded to ester}}{\text{area of N - H bonded to ester} + \text{area of N - H bonded to amide}}$$

have been determined by deconvolution of the respective FT-IR signals (see the corresponding values in Figures 5 and S6).

The areas of the FT-IR bands are related to the extinction coefficients (ϵ) as follows:

$$\text{area} = (\text{Number of hydrogen bonds}) \times (\epsilon)$$

We define the correction factor (Cf), to take into consideration the difference between the ϵ values associated with N–H bonded to ester and amide carbonyls, as:

$$Cf = \frac{\epsilon_{\text{N - H bonded to amide}}}{\epsilon_{\text{N - H bonded to ester}}}$$

Cf is extracted from the computed FT-IR spectra of **BTA Gly^{Me}** conformers, [6 - 5/1], [6 - 4/2], and [6 - 3/3].

Conformer [6 - 5/1]:

$$f = \frac{5}{5 + Cf} = 0.79 \text{ which yields } Cf = 1.33$$

Conformer [6 - 4/2]:

$$f = \frac{4}{4 + 2 \times Cf} = 0.58 \text{ which yields } Cf = 1.45$$

Conformer [6 - 3/3]:

$$f = \frac{3}{3 + 3 \times Cf} = 0.44 \text{ which yields } Cf = 1.30$$

The average Cf value is $\frac{1.33 + 1.45 + 1.30}{3} = 1.36$

Now we determine the fraction of the N–H bonded to ester in **BTA Gly** dimers according to its exp. FT-IR spectrum:

$$f = \frac{\text{number of N - H bonded to ester}}{\text{number of N - H bonded to ester} + Cf \times \text{number of N - H bonded to amide}} = 0.68 \text{ and}$$

number of N - H bonded to ester + number of N - H bonded to amide = 6 (assuming that all amide N–H are bonded)

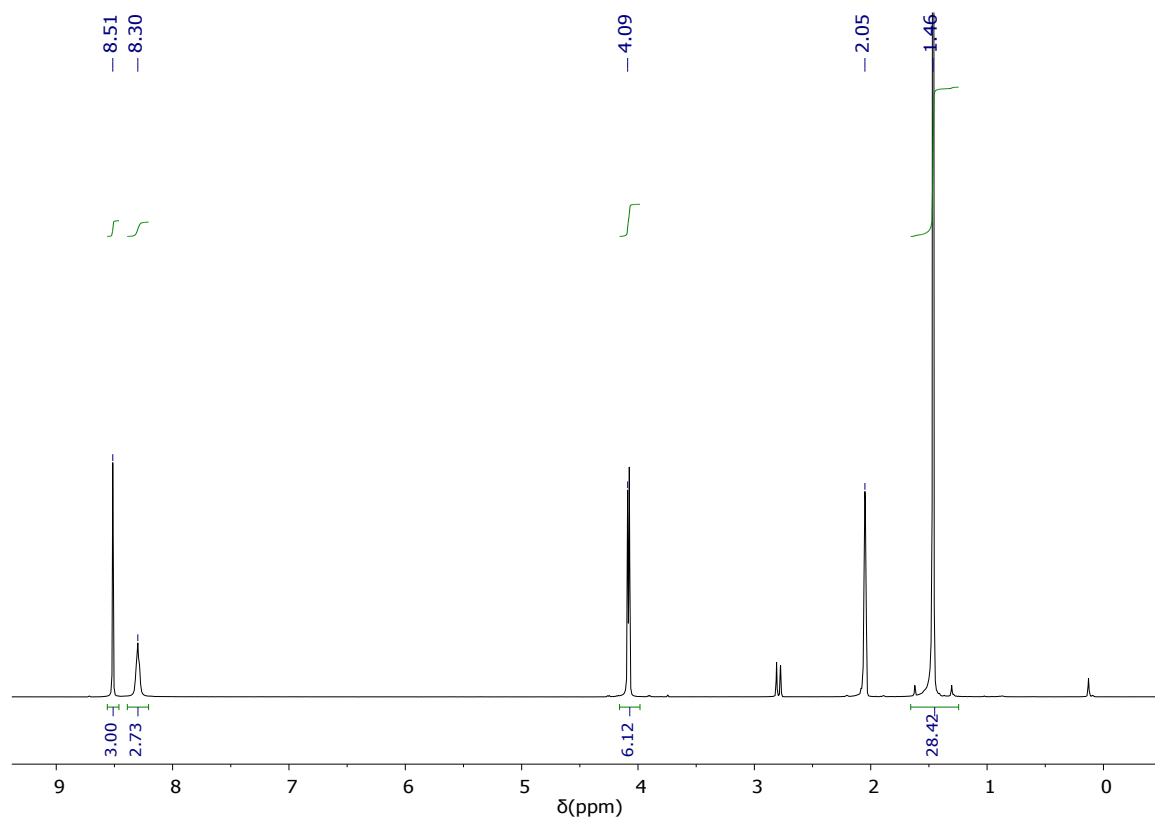
It yields the **number of N–H bonded to ester= 4.46 and that 74±2% of the HB acceptors are ester carbonyls.**

Synthesis of BTA Gly^{t-Bu}

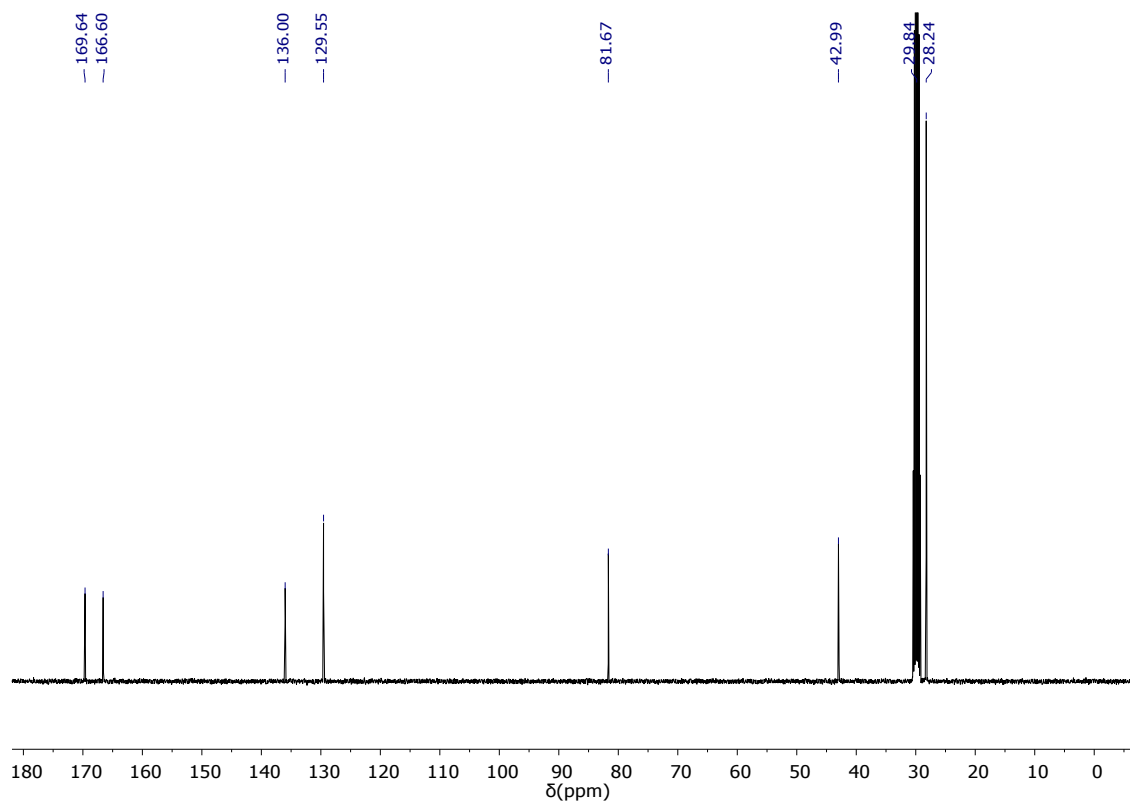
In a flame-dried round-bottom flask, benzene-1,3,5-tricarbonyl trichloride (0.25 g, 0.93 mmol, 1.0 equiv.) was dissolved in dry CH₂Cl₂ (50 mL) at room temperature under argon atmosphere. The *tert*-butyl ester HCl salt of glycine⁴ (0.56 g, 3.34 mmol, 3.6 equiv.) was then added in one portion, and the resulting mixture was cooled to 0°C with an ice/water bath. Dry Et₃N (1.0 mL, 7.1 mmol, 7.6 equiv.) was then added dropwise, the reaction was let warm to room temperature and stirred for 36 h. Brine was then added to the flask, and the crude mixture was extracted thrice with CH₂Cl₂. The combined organic phases were dried over MgSO₄, filtered, and the solvent was evaporated under reduced pressure. The product was then purified by flash column chromatography on silica gel, eluting with DCM/AcOEt 100:0–85:25 gradient yielding **BTA Gly^{t-Bu}** as a colourless solid (0.44 g, 0.80 mmol, 86% yield).

¹H NMR (acetone-d₆): δ (ppm) 8.51 (s, 3H, CH arom.), 8.30 (t, ³J= 5.5 Hz, 3H, NH), 4.09 (d, ³J= 5.5 Hz, 6H, NHCH₂), 1.46 (s, 27H, C(CH₃)₃). ¹³C{¹H} NMR (acetone-d₆): δ (ppm) 169.64 (C=O), 166.60 (C=O), 136.00 (C arom.), 129.55 (CH arom.), 81.67 (C(CH₃)₃), 42.99 (NHCH₂), 28.24 (C(CH₃)₃). HRMS (ESI, m/z): Calculated for C₅₄H₇₈N₆NaO₁₈, [M₂+Na]⁺: 1121.5270, found: 1121.5284. FT-IR (ATR, cm⁻¹) of the amorphous solid (after evaporation of the DCM/AcOEt solvent mixture): 750 (w), 847 (w), 910 (w), 943 (w), 1001 (w), 1026 (w), 1088 (w), 1152 (s), 1227 (s), 1277 (w), 1315 (w), 1335 (w), 1366 (m), 1456 (w), 1530 (m), 1639 (m), 1651 (m), 1666 (m), 1678 (m), 1719 (sh), 1728 (m), 1751 (m), 2876 (sh), 2937 (w), 2980 (w), 3069 (w), 3109 (w), 3265 (w), 3325 (w), 3362 (w), 3406 (w). FT-IR (ATR, cm⁻¹) of monocrystals of spiral-type dimers: 683 (w), 704 (w), 752 (m), 851 (m), 932 (w), 1005 (w), 1029 (w), 1095 (sh), 1154 (s), 1235 (s), 1253 (sh), 1293 (w), 1366 (s), 1375 (sh), 1396 (w), 1406 (w), 1463 (w), 1528 (m), 1666 (m), 1732 (m), 2933 (w), 2975 (w), 2999 (w), 3070 (w), 3338 (sh), 3399 (w). FT-IR (ATR, cm⁻¹) of monocrystals of the dissymmetric dimers (contaminated with spiral-type dimers): 671 (w), 700 (w), 716 (w), 733 (m), 748 (m), 837 (sh), 849 (m), 922 (w), 943 (w), 958 (sh), 1003 (w), 1024 (w), 1084 (sh), 1152 (s), 1234 (s), 1252 (sh), 1279 (m), 1306 (w), 1317 (m), 1337 (w), 1366 (s), 1406 (w), 1456 (w), 1477 (w), 1530 (m), 1555 (sh), 1595 (w), 1641 (m), 1651 (sh), 1666 (m), 1680 (m), 1726 (m), 1753 (w), 2872 (w), 2938 (w), 2982 (w), 3007 (sh), 3063 (w), 3097 (sh), 3198 (sh), 3265 (m), 3371 (m), 3395 (m), 3416 (m). FT-IR spectra (zoom on the N–H and carbonyl regions) of these solids are shown in Figure S3.

^1H NMR spectrum of BTA Gly^t-Bu (acetone -d₆)



$^{13}\text{C}\{^1\text{H}\}$ NMR spectrum of BTA Gly^t-Bu (acetone -d₆)



Computed infrared spectra (Tables S4-S14, Figure S11)

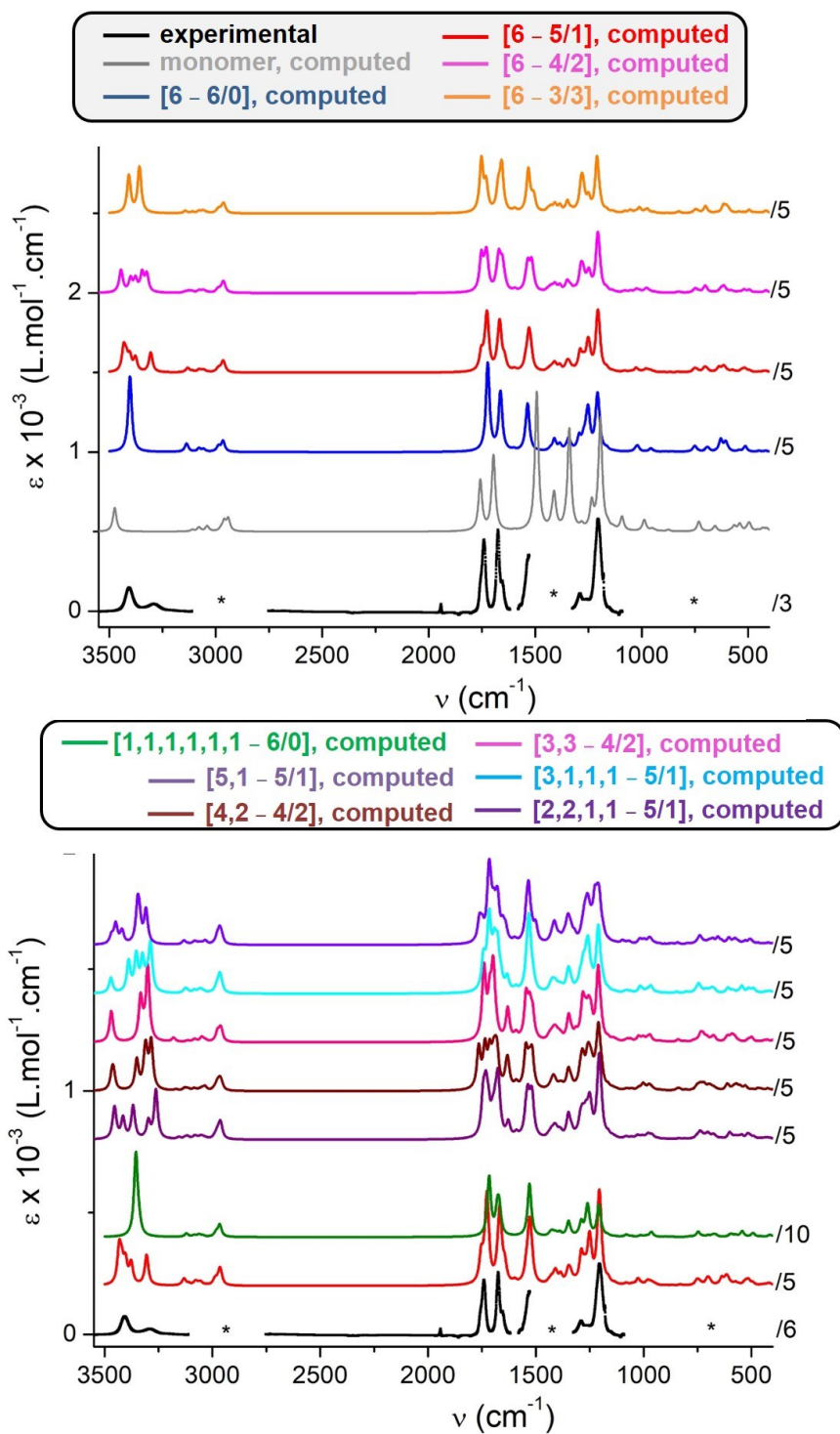


Figure S11 Full experimental (BTA Gly) and computed (BTA Gly^{Me}) FT-IR spectra for all conformations investigated in this paper. Parts of the experimental FT-IR spectrum, which are saturated, are indicated with an asterisk (*).

Table S4 Frequencies and dipole strengths of the infrared spectra of **BTA Gly^{Me}** [6-6/0] computed by the B3LYP-GD3BJ/cc-pVDZ method.

frequency cm ⁻¹	D 10 ⁻⁴⁰ esu ² cm ²	frequency cm ⁻¹	D 10 ⁻⁴⁰ esu ² cm ²	frequency cm ⁻¹	D 10 ⁻⁴⁰ esu ² cm ²	frequency cm ⁻¹	D 10 ⁻⁴⁰ esu ² cm ²	frequency cm ⁻¹	D 10 ⁻⁴⁰ esu ² cm ²
37.0	0.0	276.8	0.0	776.8	0.0	1206.7	1580.2	1541.3	0.0
37.5	352.1	277.1	0.4	777.2	0.6	1206.8	1587.5	1544.5	280.5
37.8	71.6	277.1	44.5	777.2	0.7	1207.2	0.3	1599.9	35.4
38.0	0.2	277.2	42.6	777.4	0.7	1209.0	0.0	1600.1	35.8
38.5	75.9	279.6	0.0	786.6	26.0	1209.0	0.0	1601.5	0.0
45.9	0.0	281.4	161.2	789.5	0.0	1212.6	1039.1	1601.7	0.0
52.1	0.2	297.7	464.1	857.4	28.6	1250.8	1246.5	1654.0	0.0
52.4	0.5	297.8	463.9	857.5	28.4	1251.0	1235.5	1659.2	329.6
52.7	274.8	298.8	0.1	860.1	0.0	1252.1	0.0	1663.6	1459.7
53.2	264.6	299.0	0.1	860.2	0.0	1252.3	0.1	1663.7	1461.7
57.8	140.3	326.8	24.8	884.7	13.0	1259.3	883.6	1666.4	0.1
65.7	0.0	327.0	0.1	884.9	0.0	1261.6	0.0	1666.4	0.0
69.3	235.5	350.5	735.0	890.1	0.0	1268.3	0.0	1719.3	0.0
69.5	237.3	351.0	735.9	890.1	0.0	1272.8	692.8	1722.9	2318.7
70.6	0.1	354.6	0.0	893.0	19.5	1291.9	0.0	1723.0	2318.4
77.5	0.0	355.3	0.0	893.1	19.6	1292.0	0.0	1727.1	0.1
78.0	0.0	355.6	0.0	942.3	35.3	1293.7	453.5	1727.2	0.1
79.0	361.6	356.8	371.8	943.0	0.0	1293.8	456.3	1730.4	2.4
87.9	0.4	417.7	102.5	956.2	0.0	1329.8	0.0	2965.5	2.5
89.2	0.0	417.8	105.1	957.0	290.1	1330.5	89.8	2965.5	130.7
89.8	0.0	419.5	0.0	958.4	5.0	1341.5	0.0	2965.5	14.9
90.4	22.1	419.5	0.0	958.6	0.0	1342.2	295.8	2965.6	84.6
90.6	27.4	432.9	0.0	959.2	5.6	1343.0	1.9	2965.6	92.7
95.8	0.0	433.1	17.4	959.6	0.0	1343.0	2.2	2965.7	0.1
97.6	0.0	449.4	0.2	973.2	4.6	1343.1	230.6	2987.2	36.4
97.8	0.0	449.5	93.5	973.2	4.6	1343.1	230.1	2987.3	30.0
98.5	52.4	449.7	0.3	975.1	0.0	1350.7	0.0	2987.3	44.2
99.5	55.2	449.8	91.0	975.1	0.0	1354.0	114.3	2987.3	50.6
116.0	462.5	511.7	0.0	996.4	0.0	1383.6	0.0	2987.3	0.7
117.5	0.1	511.9	0.0	997.4	0.8	1383.7	112.0	2987.4	0.1
122.1	389.3	513.5	490.0	1018.5	426.5	1383.8	0.1	3055.3	0.0
122.7	389.6	513.7	486.1	1021.7	0.0	1384.1	140.3	3055.3	10.2
125.4	71.9	543.1	199.0	1025.3	0.0	1384.3	140.6	3055.4	10.2
125.4	384.7	546.4	0.0	1025.3	0.0	1384.6	0.0	3055.4	0.0
126.0	1.2	592.4	0.1	1027.2	106.1	1404.4	12.2	3055.5	0.0
144.7	0.0	592.7	0.1	1027.3	106.6	1404.4	0.1	3055.5	7.4
154.6	0.2	593.5	82.8	1046.7	0.0	1404.5	12.9	3057.2	5.5
155.2	157.4	593.6	82.7	1048.3	6.7	1404.5	0.6	3057.2	12.5
155.3	2.4	598.0	0.0	1076.3	0.1	1404.6	0.1	3057.3	5.5
156.1	169.8	602.0	3.6	1076.5	5.6	1404.7	3.1	3057.3	8.1
157.1	21.9	605.6	1342.8	1076.5	0.1	1409.9	101.1	3057.3	8.1
159.2	0.0	624.9	0.0	1076.7	5.8	1410.0	1.4	3057.3	6.7
176.6	0.0	626.9	0.0	1127.4	9.3	1410.0	55.8	3078.4	19.6
177.7	0.0	628.3	861.4	1127.5	0.5	1410.1	8.5	3078.4	6.7
178.7	158.3	628.4	4.9	1127.6	10.1	1410.2	551.8	3078.5	28.8
179.0	135.7	629.4	857.8	1127.6	0.4	1410.2	0.2	3078.5	4.9
179.2	162.9	679.1	0.0	1127.7	0.0	1428.8	39.7	3078.5	34.7
184.0	0.0	688.3	396.1	1127.8	1.6	1428.8	2.8	3078.5	7.0
199.0	0.0	696.3	142.6	1136.7	0.0	1428.9	37.8	3135.8	7.0
199.7	0.0	696.4	141.1	1137.1	0.0	1428.9	5.0	3136.1	0.1
200.7	0.0	696.8	0.0	1137.5	1.6	1429.0	0.7	3136.4	1.6
201.6	5.9	696.9	0.0	1137.8	1.7	1429.0	33.1	3136.5	114.7
211.2	275.5	730.1	0.0	1163.7	1.4	1431.5	5.4	3136.7	19.5
211.4	266.0	733.1	30.5	1163.7	52.9	1431.7	5.3	3136.9	96.2
223.5	1.5	746.2	0.1	1163.8	1.1	1431.7	0.0	3398.8	0.1
231.4	0.0	747.8	412.2	1163.8	0.8	1431.8	0.0	3402.5	991.2
234.4	0.0	753.9	173.9	1163.8	47.9	1532.7	0.0	3403.1	984.7
234.5	0.0	754.1	176.9	1163.9	72.2	1532.9	0.0	3404.8	1.0
248.9	49.2	755.5	0.0	1199.5	497.8	1535.3	1333.9	3405.3	9.7
249.1	46.1	755.8	0.0	1200.5	0.2	1535.5	1338.5	3405.4	36.3

Table S5 Frequencies and dipole strengths of the infrared spectra of **BTA Gly^{Me}** [6-5/1] computed by the B3LYP-GD3BJ/cc-pVDZ method.

frequency cm ⁻¹	D 10 ⁻⁴⁰ esu ² cm ²	frequency cm ⁻¹	D 10 ⁻⁴⁰ esu ² cm ²	frequency cm ⁻¹	D 10 ⁻⁴⁰ esu ² cm ²	frequency cm ⁻¹	D 10 ⁻⁴⁰ esu ² cm ²	frequency cm ⁻¹	D 10 ⁻⁴⁰ esu ² cm ²
26.5	29.2	263.0	98.2	773.9	1.8	1202.1	1458.1	1536.1	170.0
30.7	74.9	269.2	27.8	775.8	0.3	1205.2	320.2	1544.9	457.8
32.1	45.2	270.5	38.1	777.9	6.3	1206.5	1178.0	1596.2	62.4
37.4	99.9	278.6	41.4	779.4	2.2	1207.4	710.0	1597.7	20.5
39.6	46.0	279.6	47.4	788.8	5.0	1209.8	916.5	1598.6	11.4
42.9	146.8	281.9	13.4	804.2	16.8	1213.4	144.2	1601.6	14.3
43.5	8.1	288.1	113.7	829.9	70.9	1241.8	120.8	1644.3	601.7
49.3	48.3	298.1	218.4	855.6	5.3	1247.8	835.5	1662.1	307.0
52.7	214.3	298.7	189.6	863.9	11.6	1251.1	573.5	1666.6	1243.2
56.5	238.5	306.3	150.6	870.0	6.6	1253.9	292.8	1667.5	834.3
59.7	15.4	316.5	20.2	870.6	9.9	1254.3	467.4	1669.7	185.1
63.5	51.2	332.8	22.6	887.0	2.2	1258.2	82.6	1676.5	361.8
66.2	51.9	340.3	113.6	889.6	7.8	1267.3	65.2	1723.5	687.2
68.7	183.4	349.1	324.2	890.7	5.5	1273.5	503.1	1726.4	1574.2
70.4	86.4	351.2	681.5	896.9	1.1	1285.0	162.9	1727.9	574.1
72.8	12.8	352.9	348.9	909.7	16.6	1288.9	244.6	1732.0	114.5
73.3	25.8	354.7	38.5	941.0	36.4	1289.2	221.8	1737.1	412.4
76.7	92.9	355.6	288.5	944.7	21.3	1290.5	691.9	1753.8	884.0
82.8	77.2	411.3	117.9	955.9	74.5	1320.0	83.0	2959.8	74.3
85.8	86.8	418.0	49.7	959.2	19.8	1330.8	36.9	2962.7	44.9
87.3	172.4	419.2	117.2	960.9	37.5	1335.3	3.6	2965.0	48.8
90.4	5.6	425.6	99.4	966.7	68.8	1337.2	98.9	2965.4	62.7
93.5	49.2	432.6	4.4	968.0	5.6	1340.5	78.1	2965.4	10.9
95.0	154.7	438.2	98.6	969.6	9.1	1341.4	177.0	2965.8	60.8
95.9	80.5	451.3	64.8	973.5	14.7	1345.5	78.4	2969.0	72.9
99.1	117.8	453.4	15.6	975.5	85.9	1348.6	176.2	2981.1	22.3
102.9	166.5	455.8	7.7	981.9	109.0	1350.8	141.2	2984.9	25.4
105.3	97.5	468.0	15.3	982.5	81.2	1353.0	169.1	2987.6	28.4
115.6	82.6	493.7	291.0	992.2	18.3	1382.1	61.7	2988.1	30.4
116.7	70.6	506.4	87.1	993.3	1.0	1384.3	90.0	2992.1	29.5
121.3	71.5	515.0	541.5	998.5	17.9	1384.5	34.4	3025.4	4.4
125.5	160.0	527.0	342.0	1008.4	24.4	1384.8	76.2	3034.9	6.1
130.4	108.4	535.0	128.3	1013.9	25.3	1385.8	88.1	3050.1	7.9
137.6	145.2	559.4	84.1	1024.2	126.1	1391.6	27.3	3052.8	6.8
143.8	442.2	560.5	11.0	1025.0	66.4	1403.6	35.9	3053.8	6.0
152.6	50.6	570.2	68.0	1027.8	181.5	1404.7	8.8	3053.8	5.2
154.6	175.8	575.4	207.1	1049.3	52.1	1405.0	43.3	3055.2	5.4
155.6	9.0	591.3	10.4	1057.7	21.3	1405.0	14.0	3055.8	8.6
159.5	32.5	594.6	99.0	1075.6	10.0	1406.2	35.0	3057.7	7.5
164.8	43.4	597.1	0.9	1075.9	6.5	1407.6	66.6	3057.9	15.6
169.6	8.3	605.8	120.4	1080.4	55.5	1408.9	54.7	3058.0	7.2
172.7	105.1	612.3	585.4	1081.3	26.4	1409.5	109.4	3066.3	10.9
175.2	97.8	620.3	388.5	1126.3	3.8	1410.7	116.4	3075.0	17.4
180.4	123.4	635.9	118.3	1128.2	2.2	1414.3	84.7	3076.6	8.2
182.1	109.5	638.1	548.5	1129.0	3.3	1420.2	47.6	3077.5	15.3
186.1	22.2	658.3	40.1	1132.6	5.7	1426.0	52.2	3077.6	19.0
189.7	68.2	681.3	29.6	1133.9	19.7	1427.1	2.2	3079.1	15.5
191.3	40.3	692.7	149.7	1134.6	1.0	1427.8	19.4	3085.1	7.5
193.7	1.5	695.6	173.9	1135.8	13.8	1428.3	40.0	3107.9	23.5
195.5	0.4	699.2	58.7	1137.5	1.0	1429.1	17.7	3111.6	8.0
201.0	29.6	703.7	187.4	1138.4	6.6	1429.4	16.6	3127.9	20.3
205.6	158.6	705.1	281.9	1141.9	8.5	1430.2	7.6	3129.6	50.7
212.2	100.5	716.3	34.8	1163.1	20.3	1431.1	14.9	3133.9	35.9
219.3	101.2	732.2	67.5	1163.2	40.4	1434.0	16.4	3134.3	25.3
227.2	17.0	741.6	128.4	1164.0	34.4	1438.6	36.8	3305.2	540.2
235.9	106.6	742.7	61.4	1165.6	63.3	1442.0	42.7	3377.0	365.1
238.8	19.0	749.5	215.1	1165.9	42.7	1516.9	280.5	3403.3	375.8
240.8	26.7	753.7	63.8	1166.5	17.4	1522.9	731.2	3420.2	315.8
246.4	200.6	755.0	102.2	1196.3	380.5	1528.6	821.5	3430.9	204.5
260.4	82.3	757.7	53.1	1200.0	4.1	1531.2	958.7	3432.8	411.1

Table S6 Frequencies and dipole strengths of the infrared spectra of **BTA Gly^{Me}** [6-4/2] computed by the B3LYP-GD3BJ/cc-pVDZ method.

frequency cm ⁻¹	D 10 ⁻⁴⁰ esu ² cm ²	frequency cm ⁻¹	D 10 ⁻⁴⁰ esu ² cm ²	frequency cm ⁻¹	D 10 ⁻⁴⁰ esu ² cm ²	frequency cm ⁻¹	D 10 ⁻⁴⁰ esu ² cm ²	frequency cm ⁻¹	D 10 ⁻⁴⁰ esu ² cm ²
25.0	32.0	263.6	72.8	774.1	2.7	1202.3	1242.9	1535.3	1214.2
27.7	60.6	264.8	65.6	774.6	3.4	1203.2	176.1	1544.8	277.3
30.2	68.6	268.7	16.3	778.1	4.8	1205.8	929.2	1594.0	75.3
34.6	89.8	270.4	63.4	780.4	1.0	1207.8	609.8	1596.9	19.0
39.0	37.7	276.7	34.0	788.0	8.2	1208.7	1545.8	1598.1	17.6
42.0	50.4	282.5	17.5	810.1	20.2	1218.0	100.3	1600.7	7.8
42.7	55.9	291.8	143.8	827.0	102.5	1240.2	152.8	1643.7	285.5
46.3	60.6	294.6	98.9	832.6	31.5	1246.9	756.8	1654.3	1280.1
51.5	73.2	300.7	127.5	861.1	7.6	1248.6	64.9	1665.6	468.4
53.4	122.6	308.4	98.4	869.7	0.6	1251.1	295.2	1670.9	794.0
55.7	104.5	310.8	52.0	871.3	0.8	1256.9	217.2	1672.5	569.2
60.7	27.1	335.7	29.3	880.2	5.9	1266.5	112.6	1680.0	321.3
65.9	78.0	340.3	126.0	888.0	2.5	1270.3	84.5	1726.3	664.3
67.0	57.5	343.4	59.9	894.1	0.2	1274.6	645.6	1728.9	258.2
68.0	104.1	347.6	342.5	897.9	2.7	1279.8	252.6	1729.8	955.3
72.5	80.6	350.7	770.3	913.4	16.1	1281.8	468.8	1739.3	444.4
76.5	74.7	352.2	312.6	936.8	32.7	1286.2	434.3	1753.2	1238.5
78.6	86.1	354.4	112.7	938.5	46.5	1287.3	573.7	1753.5	518.1
83.8	113.8	413.2	205.5	955.8	5.9	1314.8	83.2	2959.8	72.5
86.9	67.5	417.8	65.5	957.9	56.2	1330.1	82.6	2960.8	67.7
89.7	19.7	418.4	246.3	961.9	44.8	1331.0	10.1	2962.8	43.9
90.3	76.1	421.7	26.1	967.5	2.4	1335.6	3.5	2965.2	25.5
92.0	34.5	435.3	29.9	970.8	49.8	1336.0	176.1	2965.7	45.6
92.5	162.4	450.2	23.7	973.7	78.1	1338.3	20.5	2966.8	48.9
100.4	109.0	453.6	4.1	975.0	59.6	1346.7	213.6	2968.2	76.1
102.0	166.0	456.0	31.6	978.1	97.2	1349.6	140.2	2982.1	21.6
102.7	153.1	462.6	75.5	981.0	84.3	1350.8	168.4	2982.4	19.1
107.4	41.0	470.1	22.4	983.6	51.6	1352.8	167.8	2988.5	32.0
115.6	112.0	492.5	299.7	984.8	25.5	1383.0	80.5	2989.4	30.2
120.3	49.8	498.2	228.4	992.4	9.5	1384.2	87.4	2992.4	27.9
123.5	17.2	518.1	468.2	996.5	11.0	1384.7	62.6	3026.3	4.2
130.4	112.6	528.1	117.3	1007.6	23.1	1384.9	60.8	3036.7	5.0
133.7	124.2	545.7	117.4	1010.8	55.2	1386.2	75.0	3036.8	5.3
141.1	128.8	560.2	45.6	1011.1	72.4	1393.3	23.0	3050.4	8.3
148.8	302.8	562.2	7.6	1024.5	222.5	1404.2	32.7	3052.7	7.0
150.6	315.0	565.2	4.1	1029.4	55.6	1404.3	26.0	3053.8	8.8
154.5	74.2	572.0	60.9	1051.0	133.9	1405.0	44.4	3054.5	5.8
158.5	82.3	580.1	249.5	1063.0	15.3	1406.6	90.0	3055.2	6.1
166.2	49.1	595.5	26.0	1075.2	8.5	1406.9	49.8	3057.4	8.6
168.7	15.9	596.5	63.0	1075.7	11.2	1407.4	57.6	3059.3	14.9
174.2	71.5	605.0	52.0	1077.7	63.1	1408.6	68.9	3061.0	13.6
176.3	184.0	610.7	129.7	1082.8	60.1	1409.3	59.6	3065.2	11.5
178.0	111.3	614.4	738.2	1128.9	2.5	1416.0	64.2	3075.4	17.0
179.3	120.1	627.4	481.8	1130.5	2.6	1420.9	46.3	3077.3	7.9
185.8	30.6	640.4	43.5	1132.6	3.2	1425.0	31.1	3078.0	14.0
186.7	15.1	661.8	59.9	1134.3	15.4	1425.4	25.4	3078.2	14.5
190.5	19.6	683.7	22.5	1134.6	2.9	1426.0	64.2	3079.1	7.4
191.4	10.0	695.4	115.3	1134.9	20.3	1426.5	21.4	3084.6	8.2
194.3	3.3	698.7	177.4	1135.1	5.5	1428.1	37.3	3110.0	11.2
195.2	61.3	700.8	224.1	1135.6	22.9	1428.4	14.2	3112.0	21.9
196.2	3.3	702.6	205.2	1136.4	0.9	1431.3	12.9	3113.4	11.4
206.9	147.5	704.9	224.0	1143.6	17.3	1431.9	30.2	3125.7	29.7
212.2	97.6	713.0	16.2	1163.0	30.7	1433.7	12.3	3130.7	24.0
219.3	105.6	730.1	124.4	1165.0	68.8	1438.9	39.4	3144.6	24.7
230.3	7.3	732.9	18.1	1165.6	39.1	1440.7	43.3	3323.6	474.9
238.5	86.2	743.0	79.3	1166.1	7.7	1442.2	42.9	3345.5	500.1
241.0	115.0	747.6	308.9	1166.1	53.2	1507.9	242.7	3376.6	334.3
243.9	231.0	750.9	97.5	1166.8	15.2	1515.3	399.4	3399.8	345.9
256.4	82.1	754.5	33.4	1195.6	330.7	1518.0	1142.9	3443.9	449.3
260.4	125.5	757.7	43.5	1198.4	9.4	1530.8	289.6	3447.7	150.0

Table S7 Frequencies and dipole strengths of the infrared spectra of **BTA Gly^{Me}** [6-3/3] computed by the B3LYP-GD3BJ/cc-pVDZ method.

frequency cm ⁻¹	D 10 ⁻⁴⁰ esu ² cm ²	frequency cm ⁻¹	D 10 ⁻⁴⁰ esu ² cm ²	frequency cm ⁻¹	D 10 ⁻⁴⁰ esu ² cm ²	frequency cm ⁻¹	D 10 ⁻⁴⁰ esu ² cm ²	frequency cm ⁻¹	D 10 ⁻⁴⁰ esu ² cm ²
23.8	19.5	264.5	5.2	773.2	3.7	1203.5	225.8	1532.5	1239.0
24.2	19.1	265.4	63.8	773.3	3.7	1203.7	217.6	1543.9	47.3
31.3	108.8	265.6	63.9	779.7	3.7	1210.4	1729.2	1595.6	61.3
33.9	32.3	268.6	86.9	780.0	3.9	1210.4	1741.5	1595.7	61.2
34.4	30.1	273.9	5.3	786.9	1.2	1211.0	276.7	1598.3	15.6
39.4	19.3	274.1	6.8	806.4	6.2	1220.4	1.1	1598.6	14.7
43.2	37.0	292.3	116.0	826.1	101.6	1242.1	0.1	1643.1	13.9
43.7	31.3	292.4	117.2	826.2	101.4	1249.4	455.6	1657.4	1227.7
45.0	4.4	307.8	104.4	836.7	1.1	1249.6	450.3	1657.5	1229.1
50.6	51.4	308.1	102.7	871.7	0.1	1251.1	2.4	1670.3	295.6
51.0	55.1	310.4	0.6	871.7	0.1	1265.3	128.6	1674.1	497.8
61.4	0.5	335.3	131.1	879.2	11.0	1269.8	63.9	1674.2	500.1
63.8	21.2	341.8	46.9	879.3	11.1	1270.0	62.4	1730.0	445.7
64.3	18.6	341.8	51.2	895.3	0.0	1275.7	800.7	1730.1	445.7
65.2	211.6	344.4	23.4	898.7	3.2	1278.7	465.0	1731.4	508.4
73.6	127.3	348.2	640.5	898.8	3.2	1279.0	464.0	1752.7	1308.8
73.8	128.7	348.5	638.3	937.0	27.3	1285.5	638.0	1752.7	1323.3
83.1	151.5	353.6	100.3	943.8	70.5	1285.9	633.2	1753.2	49.9
88.5	40.1	415.0	219.3	955.5	10.9	1311.8	46.6	2960.5	71.5
88.6	64.8	415.4	220.3	957.4	12.7	1329.3	0.1	2960.6	66.9
89.3	95.4	421.5	55.8	962.6	4.0	1329.6	58.4	2960.8	56.8
89.6	124.6	421.6	58.1	965.1	3.5	1329.7	59.1	2967.3	40.1
91.6	142.8	439.0	72.1	972.1	127.4	1336.0	4.3	2967.5	42.0
92.8	4.9	453.9	0.6	973.9	93.8	1337.1	11.4	2967.6	58.7
98.4	97.8	454.8	37.7	974.0	93.1	1348.8	336.2	2982.5	25.0
99.0	93.5	454.9	38.3	974.7	0.9	1348.9	335.5	2982.6	27.0
106.4	104.4	469.1	68.1	982.9	55.0	1350.3	33.2	2982.7	6.5
106.8	105.1	469.5	70.2	983.0	54.3	1351.9	5.2	2989.2	37.4
111.7	7.1	495.6	296.8	984.5	10.4	1383.5	88.8	2989.3	42.4
127.2	89.3	495.8	290.7	992.2	16.2	1383.6	85.8	2989.4	7.1
127.7	88.7	523.1	131.2	997.3	2.5	1383.8	64.1	3037.2	3.8
135.2	262.8	543.5	104.3	1009.5	35.0	1384.1	64.0	3037.3	3.2
139.0	98.2	543.8	103.4	1009.6	34.8	1384.2	59.2	3037.3	6.9
141.3	51.6	560.7	3.0	1010.9	394.7	1385.3	53.9	3053.5	8.6
141.6	50.1	565.0	13.2	1028.0	48.7	1404.4	18.9	3053.6	8.7
150.8	480.2	565.1	13.4	1028.1	48.6	1404.5	22.0	3053.8	8.7
151.5	139.5	567.1	0.5	1052.6	232.6	1404.6	43.9	3055.9	6.3
151.9	116.3	590.7	181.7	1063.3	8.7	1407.3	36.3	3056.2	6.4
154.3	3.4	590.8	180.5	1075.6	4.9	1407.5	33.2	3056.2	6.2
174.3	53.8	600.3	141.1	1075.7	4.0	1407.8	133.1	3062.2	15.6
174.5	55.7	601.8	311.6	1078.0	62.1	1408.4	82.9	3062.3	15.2
176.4	172.0	602.0	317.8	1078.2	60.7	1408.4	72.2	3062.4	10.2
179.5	191.3	608.9	11.6	1131.1	4.0	1408.4	55.2	3077.9	15.0
179.6	181.4	616.0	1063.8	1131.3	4.3	1424.6	26.1	3078.0	14.8
186.0	3.8	648.5	40.1	1131.5	0.3	1424.7	25.2	3078.1	13.3
187.8	23.1	651.0	37.2	1134.5	13.1	1425.5	18.1	3079.5	7.2
188.2	26.7	684.5	21.3	1134.7	6.0	1425.9	37.6	3079.7	7.0
192.2	60.3	698.6	270.2	1135.2	4.2	1426.0	56.7	3079.8	6.0
192.8	4.6	699.2	22.3	1135.4	37.6	1427.0	37.1	3109.2	7.0
193.5	4.7	699.4	134.0	1135.5	27.2	1427.2	40.8	3110.0	12.7
194.2	3.2	701.2	243.5	1136.7	2.9	1432.0	5.1	3110.3	18.0
205.6	37.3	701.5	243.0	1137.0	4.3	1432.3	34.9	3141.2	2.9
217.8	128.3	713.6	0.1	1165.5	12.3	1432.4	35.0	3142.1	30.8
218.7	131.7	732.5	92.9	1165.7	61.7	1441.3	58.5	3142.4	33.3
234.6	26.6	733.0	8.4	1165.8	64.8	1441.4	61.7	3357.4	424.8
239.5	198.6	733.1	9.0	1166.1	2.5	1441.4	15.5	3358.2	424.5
239.8	199.2	745.8	407.5	1166.7	13.8	1506.2	408.5	3358.9	392.7
254.5	58.9	749.6	9.2	1166.7	13.8	1506.8	406.1	3407.7	144.7
258.9	147.1	755.9	37.1	1195.8	272.6	1515.2	231.5	3408.0	438.4
259.1	144.3	755.9	37.2	1199.7	12.5	1532.1	1238.2	3408.4	412.6

Table S8 Frequencies and dipole strengths of the infrared spectra of **BTA Gly^{Me} [5,1-5/1]** computed by the B3LYP-GD3BJ/cc-pVDZ method.

frequency cm ⁻¹	D 10 ⁻⁴⁰ esu ² cm ²	frequency cm ⁻¹	D 10 ⁻⁴⁰ esu ² cm ²	frequency cm ⁻¹	D 10 ⁻⁴⁰ esu ² cm ²	frequency cm ⁻¹	D 10 ⁻⁴⁰ esu ² cm ²	frequency cm ⁻¹	D 10 ⁻⁴⁰ esu ² cm ²
23.8	120.7	259.2	116.2	770.8	7.2	1200.4	500.3	1537.5	1173.2
25.2	28.5	266.8	93.5	776.2	5.9	1204.4	1322.2	1546.8	585.0
26.5	115.5	272.1	39.4	780.7	1.6	1204.9	326.3	1589.1	145.8
35.8	50.1	277.8	69.1	782.5	22.8	1208.5	1319.1	1596.3	6.7
37.4	146.6	279.3	24.6	797.5	8.4	1210.6	705.8	1599.7	3.6
40.9	69.8	283.4	34.2	810.1	53.0	1216.8	79.3	1600.6	13.3
43.1	42.3	295.5	124.1	836.6	80.7	1240.9	142.1	1627.7	529.8
46.8	199.8	298.8	103.9	859.0	6.8	1247.4	798.1	1663.6	84.5
50.4	108.6	301.8	256.1	865.7	4.0	1249.4	35.8	1673.3	1125.9
52.2	74.7	307.3	11.2	871.8	5.1	1253.1	787.0	1677.8	790.7
56.9	157.6	330.3	33.5	874.5	11.3	1254.4	61.1	1679.3	226.0
60.7	52.9	336.5	109.6	887.1	2.4	1264.4	284.9	1689.4	708.2
63.3	128.2	345.9	548.2	894.4	4.7	1265.4	239.6	1700.9	519.4
65.7	105.7	350.7	401.4	899.9	11.6	1270.6	425.8	1719.5	724.0
69.5	58.3	351.1	331.4	905.2	12.1	1278.7	267.3	1729.6	752.6
71.8	161.6	355.4	26.4	911.0	9.8	1284.2	129.2	1732.7	606.1
72.7	33.6	363.6	562.7	929.6	30.7	1284.5	475.6	1739.8	416.3
75.8	46.4	370.8	471.9	937.2	33.1	1294.2	649.8	1745.3	976.2
78.2	145.3	397.8	13.5	953.0	18.7	1313.7	52.9	2958.6	64.6
81.4	78.5	416.1	96.5	954.6	12.3	1332.2	79.8	2962.0	74.6
82.0	310.4	422.7	71.2	959.4	74.8	1333.9	42.7	2962.1	29.4
85.7	20.8	432.3	22.0	961.4	139.0	1336.7	146.1	2962.3	63.5
89.3	4.6	433.7	153.0	968.3	11.1	1338.6	3.9	2963.5	43.0
90.5	142.0	441.5	19.1	973.1	64.4	1347.0	131.0	2966.4	29.9
95.5	26.3	448.3	4.6	977.6	102.2	1348.0	109.7	2968.2	76.4
99.5	92.0	449.2	7.4	979.5	90.9	1348.8	544.6	2975.0	23.3
100.2	92.8	453.9	99.1	983.8	10.6	1350.9	50.2	2977.4	22.2
101.2	150.3	470.7	40.3	985.4	33.4	1352.2	159.7	2978.2	31.8
109.1	38.6	488.9	252.1	986.0	33.7	1382.1	76.9	2982.0	43.3
116.0	78.3	492.6	13.7	993.0	17.1	1385.5	75.4	2991.2	29.7
120.3	6.5	506.1	285.3	998.0	4.3	1388.4	54.7	3026.7	4.8
123.1	26.5	517.8	525.3	1002.9	90.0	1390.0	61.0	3028.6	6.9
125.9	209.8	544.6	356.3	1009.5	56.2	1393.7	19.1	3035.9	6.8
137.3	18.6	555.5	93.7	1013.5	30.6	1395.8	36.7	3038.6	7.7
146.0	163.9	561.3	121.0	1020.7	27.0	1402.6	80.1	3041.9	7.5
151.1	395.2	572.3	106.9	1029.2	178.3	1406.5	55.7	3044.5	16.2
161.7	85.0	574.2	111.2	1053.6	44.3	1407.0	59.1	3050.3	9.6
165.0	84.6	581.4	29.2	1056.0	52.0	1409.0	38.1	3051.4	12.9
166.4	10.2	588.0	67.4	1073.5	38.0	1409.4	36.8	3052.0	8.2
167.9	8.1	594.7	114.7	1077.3	10.8	1411.3	59.6	3056.5	8.6
172.0	96.1	601.1	432.0	1083.0	3.7	1412.9	38.9	3056.9	12.5
173.5	16.4	604.1	28.2	1083.2	86.3	1415.1	131.0	3065.2	10.4
174.9	30.2	605.1	129.1	1126.0	9.5	1415.5	28.3	3074.0	19.5
178.3	137.0	640.6	83.9	1126.4	2.3	1420.7	53.6	3079.4	13.2
180.0	52.6	664.1	98.0	1130.3	14.1	1423.9	7.6	3082.2	15.2
181.2	21.3	673.6	208.1	1131.0	3.9	1425.4	23.3	3083.2	8.4
185.3	44.8	679.8	174.8	1132.9	2.7	1426.2	18.5	3084.8	14.6
190.0	6.1	693.8	124.5	1134.3	1.3	1426.7	39.1	3086.2	3.5
190.8	1.1	698.7	52.5	1134.9	3.2	1427.7	50.8	3111.1	5.0
197.9	72.1	703.3	212.3	1135.1	1.7	1428.6	39.5	3113.0	21.8
199.0	3.7	703.4	125.5	1138.3	9.2	1430.0	5.0	3115.1	8.2
202.2	35.3	714.9	146.8	1144.3	88.6	1431.9	15.5	3118.5	15.0
208.2	156.1	721.0	15.1	1161.4	20.3	1433.4	17.7	3125.6	29.2
220.7	75.3	726.8	150.8	1163.3	27.5	1433.8	24.6	3154.7	36.5
231.1	55.0	736.8	373.4	1164.2	70.6	1439.1	36.3	3262.1	886.3
237.1	57.7	739.9	119.3	1165.5	50.6	1442.0	50.5	3296.7	308.1
238.3	95.5	743.5	21.2	1167.5	18.7	1512.6	208.3	3367.9	577.8
241.4	9.2	745.0	60.0	1170.4	0.6	1517.1	936.3	3414.7	355.8
249.9	65.2	751.7	105.8	1195.9	349.0	1522.5	637.1	3453.1	413.9
252.5	189.6	756.3	91.1	1199.8	79.9	1533.3	233.8	3457.4	152.6

Table S9 Frequencies and dipole strengths of the infrared spectra of **BTA Gly^{Me} [4,2-4/2]** computed by the B3LYP-GD3BJ/cc-pVDZ method.

frequency cm ⁻¹	D 10 ⁻⁴⁰ esu ² cm ²	frequency cm ⁻¹	D 10 ⁻⁴⁰ esu ² cm ²	frequency cm ⁻¹	D 10 ⁻⁴⁰ esu ² cm ²	frequency cm ⁻¹	D 10 ⁻⁴⁰ esu ² cm ²	frequency cm ⁻¹	D 10 ⁻⁴⁰ esu ² cm ²
22.6	108.6	256.1	106.9	768.5	19.7	1200.1	259.3	1540.7	232.5
26.5	205.9	262.4	29.8	776.1	8.3	1209.1	1866.2	1547.2	1284.5
28.7	22.2	272.3	30.0	779.6	6.3	1211.2	741.5	1590.1	175.7
32.5	44.3	274.7	119.5	780.4	0.9	1216.2	135.9	1592.2	2.4
39.0	3.7	280.3	44.8	800.2	19.0	1221.8	379.1	1597.9	19.6
40.9	82.5	286.3	43.9	806.3	53.1	1229.6	110.8	1598.5	13.1
41.3	2.9	288.3	190.1	832.9	117.4	1237.4	344.1	1629.6	740.4
47.5	200.9	298.6	40.5	842.7	119.2	1244.9	640.9	1636.0	502.6
48.5	65.1	303.4	34.3	856.3	14.1	1251.4	257.1	1679.1	497.6
51.2	109.3	314.3	119.2	870.7	5.5	1253.7	284.2	1680.3	509.6
53.6	76.7	337.7	190.5	873.1	2.3	1257.1	436.5	1687.9	621.5
57.6	13.2	338.1	92.2	874.5	3.4	1260.1	197.7	1696.6	751.3
59.5	202.5	342.5	600.1	886.3	3.9	1261.5	154.0	1705.5	158.2
62.2	31.2	348.4	270.2	892.6	2.2	1262.9	454.0	1714.6	1059.4
65.7	115.1	352.1	315.8	903.2	14.7	1278.7	569.8	1735.6	1151.6
66.4	112.8	354.5	44.8	906.5	10.2	1285.8	843.7	1740.3	204.5
73.6	106.4	362.6	439.4	924.3	3.0	1288.2	118.6	1763.3	646.7
74.9	71.1	369.3	569.7	925.5	43.4	1295.1	433.1	1766.1	730.6
79.2	121.1	395.1	21.7	941.4	19.0	1312.8	21.1	2955.9	28.1
82.3	79.6	399.5	46.5	946.5	6.5	1318.0	16.6	2958.8	70.3
82.7	104.3	416.8	71.4	956.7	34.7	1335.8	113.6	2962.9	32.3
84.6	131.0	425.2	235.1	959.2	67.3	1337.5	87.6	2964.7	43.6
86.7	73.8	445.4	50.0	970.5	172.9	1338.1	25.1	2965.3	35.7
91.4	40.9	446.7	28.6	974.9	51.4	1342.5	62.2	2968.6	71.7
94.1	31.9	457.0	52.4	975.7	29.6	1346.8	161.7	2975.3	20.9
101.4	44.2	458.9	130.2	977.4	91.4	1348.1	30.6	2976.4	27.9
103.2	128.5	469.4	64.9	983.5	31.9	1349.8	450.9	2977.0	25.3
104.3	15.7	471.9	164.7	990.3	13.1	1351.9	147.3	2978.3	21.3
114.3	1.2	496.1	133.7	992.7	23.7	1376.9	50.0	2980.1	30.6
118.0	11.2	509.2	30.9	997.0	16.1	1378.1	7.6	2989.6	30.2
118.6	13.9	527.4	397.1	1000.8	137.6	1380.7	85.8	3030.1	9.4
121.1	23.8	529.7	90.8	1003.4	219.8	1387.2	72.0	3030.7	2.4
123.9	11.5	545.1	95.0	1011.5	6.2	1391.6	56.8	3034.1	34.7
129.7	217.7	552.0	150.1	1013.9	14.3	1396.7	28.8	3035.6	4.3
142.0	58.1	556.5	201.8	1021.0	25.0	1406.5	46.7	3036.5	22.3
144.8	590.7	568.1	226.9	1023.1	107.2	1409.6	62.4	3039.6	5.8
156.7	17.3	572.1	249.8	1049.4	19.4	1410.2	23.3	3044.5	6.1
160.6	119.7	580.1	84.4	1056.4	65.9	1410.6	28.3	3047.0	13.3
161.9	14.5	582.6	90.9	1070.7	18.7	1413.4	6.4	3051.4	9.7
168.9	82.2	583.9	115.0	1075.0	30.3	1416.0	93.7	3054.0	8.5
170.8	21.2	597.9	39.1	1082.1	27.6	1416.6	36.7	3054.2	8.0
173.3	34.3	607.9	170.6	1082.5	23.5	1417.8	34.4	3064.9	10.3
175.8	55.8	612.9	484.5	1123.6	16.5	1418.1	113.6	3081.3	11.3
177.5	32.5	648.6	22.0	1127.0	2.0	1420.0	36.5	3083.0	8.3
178.0	6.1	655.3	39.9	1127.1	1.4	1421.2	60.1	3084.2	13.0
181.2	14.9	670.9	171.8	1129.4	16.2	1422.8	12.4	3086.7	0.7
188.8	74.2	678.3	65.7	1130.0	15.6	1423.2	4.2	3087.8	10.3
189.7	67.3	686.1	188.5	1133.1	1.8	1424.9	34.6	3110.2	20.5
190.8	119.7	694.4	101.1	1134.2	2.9	1425.3	63.2	3116.8	4.3
195.2	30.2	697.5	221.2	1134.8	0.6	1425.9	3.2	3117.0	10.3
197.5	53.8	702.9	45.8	1143.0	22.1	1426.2	12.4	3120.2	5.7
202.6	77.3	711.7	35.2	1144.3	51.7	1427.2	0.8	3128.4	22.2
210.4	96.8	716.7	258.1	1161.8	16.4	1429.0	16.5	3129.7	20.5
211.5	112.9	724.1	247.8	1162.5	9.5	1431.1	33.9	3168.2	21.3
230.6	111.5	731.9	123.4	1163.5	28.4	1433.1	19.5	3284.0	840.1
235.5	12.1	737.9	279.3	1164.5	26.2	1439.3	33.6	3305.0	264.8
239.8	30.0	746.2	164.1	1165.4	58.3	1515.5	369.6	3311.7	578.6
247.0	27.5	752.1	74.8	1171.2	16.1	1518.1	915.5	3350.8	523.4
250.5	232.0	752.9	42.1	1194.6	343.5	1525.9	114.2	3459.5	311.5
253.8	30.2	754.7	125.0	1198.2	143.5	1530.8	616.9	3466.6	189.9

Table S10 Frequencies and dipole strengths of the infrared spectra of **BTA Gly^{Me} [3,3-4/2]** computed by the B3LYP-GD3BJ/cc-pVDZ method.

frequency cm ⁻¹	D 10 ⁻⁴⁰ esu ² cm ²	frequency cm ⁻¹	D 10 ⁻⁴⁰ esu ² cm ²	frequency cm ⁻¹	D 10 ⁻⁴⁰ esu ² cm ²	frequency cm ⁻¹	D 10 ⁻⁴⁰ esu ² cm ²	frequency cm ⁻¹	D 10 ⁻⁴⁰ esu ² cm ²
22.5	54.9	261.1	2.2	768.6	72.1	1199.9	415.5	1536.5	169.6
22.7	34.0	261.3	405.1	771.3	21.4	1203.2	53.4	1545.5	1539.5
28.9	70.3	272.9	17.8	777.8	4.8	1210.5	2486.3	1590.8	199.9
34.1	20.2	275.1	0.6	778.9	0.2	1211.8	508.0	1592.4	0.2
34.8	145.1	280.7	7.7	803.2	11.8	1215.4	327.4	1598.3	17.3
40.5	68.7	283.2	292.0	810.1	50.9	1216.3	56.3	1598.8	19.2
41.5	5.9	288.0	54.4	839.3	123.8	1243.1	27.9	1630.4	1046.9
42.9	77.5	294.5	18.7	839.7	60.2	1244.9	896.7	1631.6	95.1
47.9	56.2	307.5	44.3	872.3	2.5	1252.3	84.5	1686.0	109.4
50.5	186.9	313.9	120.0	872.5	0.3	1254.1	245.8	1686.9	187.0
52.2	137.3	334.7	74.0	874.5	25.0	1255.9	518.4	1697.5	1585.9
56.5	38.7	335.6	259.4	877.8	0.3	1257.3	227.1	1699.1	758.2
60.2	0.1	346.4	52.8	893.5	3.7	1267.6	291.4	1706.2	53.6
61.1	105.6	347.6	178.1	894.3	8.3	1269.2	503.8	1714.0	1265.2
65.6	88.0	352.6	754.3	904.1	19.2	1280.0	318.9	1734.6	120.6
66.2	0.7	353.2	14.9	907.7	5.7	1282.1	1079.0	1735.0	221.0
68.3	179.4	363.0	562.1	923.2	0.8	1285.9	248.4	1741.3	2133.6
77.7	54.8	369.5	427.4	924.0	63.2	1287.5	158.3	1743.0	33.4
77.7	60.3	399.6	200.3	938.2	4.6	1312.9	3.3	2959.1	90.2
81.1	16.8	402.7	5.1	939.7	10.7	1314.2	283.4	2959.2	37.4
85.2	180.6	425.9	199.6	949.4	10.5	1334.0	11.2	2961.8	53.0
89.9	329.1	427.8	46.3	949.9	2.0	1334.3	151.8	2961.9	32.5
90.8	38.3	440.3	88.5	968.3	123.1	1345.1	68.0	2963.4	57.1
93.5	0.0	442.4	36.0	968.5	41.9	1346.3	147.2	2963.4	10.8
94.4	46.2	446.1	30.5	971.4	173.2	1346.4	377.4	2975.5	50.3
99.7	15.8	447.6	1.3	974.9	41.9	1348.4	20.0	2975.5	22.6
100.9	0.0	463.2	27.1	982.6	81.5	1349.6	458.2	2975.6	41.8
102.8	54.9	463.7	36.3	983.1	49.9	1350.7	0.6	2975.8	27.3
110.3	27.7	498.0	4.5	994.3	22.4	1382.6	127.8	2978.4	32.7
116.2	9.9	498.9	520.9	995.7	5.5	1382.7	9.6	2978.5	14.9
118.5	3.4	514.2	250.2	1001.7	11.5	1391.9	49.6	3029.7	12.4
120.7	2.3	515.5	6.7	1002.2	200.5	1392.5	91.9	3030.1	0.2
124.3	8.9	557.9	0.0	1012.2	18.4	1392.7	44.8	3033.7	8.0
134.3	214.4	559.8	74.0	1013.2	22.8	1398.1	28.1	3033.9	9.1
142.3	0.1	574.4	145.6	1023.6	233.1	1404.6	132.1	3039.7	1.3
147.0	590.1	574.9	90.9	1024.1	44.7	1404.8	52.7	3039.7	10.0
158.7	34.7	580.9	215.2	1058.4	2.0	1409.7	103.8	3048.0	10.0
164.7	273.0	584.2	63.5	1059.3	104.4	1409.7	42.0	3048.1	14.1
169.8	10.4	591.7	513.2	1072.8	95.9	1410.4	21.6	3048.9	4.4
172.9	125.4	594.6	7.3	1073.0	0.9	1410.5	29.4	3049.0	27.9
174.1	5.8	609.4	249.6	1081.9	2.1	1417.3	0.4	3051.4	18.2
175.0	25.9	609.5	177.1	1082.9	45.9	1417.4	161.6	3051.5	12.3
178.1	98.5	617.2	145.3	1126.3	5.6	1418.1	91.6	3079.5	15.9
178.6	1.4	645.3	7.8	1126.4	37.8	1418.5	10.6	3079.5	14.7
180.8	2.7	672.0	266.4	1127.2	1.3	1423.4	0.0	3085.3	19.7
180.8	6.8	672.6	51.7	1127.2	0.3	1424.0	4.5	3085.3	4.8
187.3	134.0	677.7	211.0	1130.2	3.7	1425.9	0.4	3088.7	1.0
192.1	121.1	687.4	123.8	1130.4	4.0	1426.1	17.7	3088.9	1.0
193.8	11.9	702.1	28.3	1137.5	1.3	1427.9	5.2	3113.6	8.7
195.6	4.1	704.8	166.7	1137.5	1.9	1428.1	88.0	3113.7	4.3
196.2	4.3	710.1	153.8	1140.6	97.8	1430.0	50.9	3116.6	5.2
198.8	0.8	712.6	4.9	1141.2	0.1	1430.4	15.4	3116.9	5.5
207.1	68.8	723.0	38.4	1162.1	14.9	1433.9	19.1	3179.8	24.2
208.8	149.9	723.9	383.2	1162.6	12.3	1434.0	32.0	3180.0	51.2
230.5	0.7	729.0	54.7	1165.7	71.4	1439.8	70.5	3299.4	499.1
232.6	89.8	733.8	32.2	1165.8	16.7	1439.9	40.6	3300.5	825.8
239.1	161.3	735.1	369.8	1170.5	0.2	1512.4	180.1	3319.7	73.6
242.8	38.1	738.4	175.0	1170.7	0.4	1515.5	752.9	3333.3	743.4
251.1	63.2	753.6	27.9	1196.6	2.8	1528.1	794.8	3468.9	390.3
254.0	13.7	754.3	48.4	1197.0	148.6	1528.6	283.1	3469.1	136.9

Table S11 Frequencies and dipole strengths of the infrared spectra of **BTA Gly^{Me}** [3,1,1,1-5/1] computed by the B3LYP-GD3BJ/cc-pVDZ method.

frequency cm ⁻¹	D 10 ⁻⁴⁰ esu ² cm ²	frequency cm ⁻¹	D 10 ⁻⁴⁰ esu ² cm ²	frequency cm ⁻¹	D 10 ⁻⁴⁰ esu ² cm ²	frequency cm ⁻¹	D 10 ⁻⁴⁰ esu ² cm ²	frequency cm ⁻¹	D 10 ⁻⁴⁰ esu ² cm ²
17.4	53.9	254.6	180.9	767.7	31.1	1199.9	75.1	1534.1	1616.3
22.1	536.4	264.1	91.1	777.2	6.3	1206.5	369.1	1543.3	518.6
24.5	21.4	272.5	5.8	779.9	6.5	1209.8	1800.7	1592.5	110.9
27.3	10.2	280.3	47.2	786.4	16.0	1211.6	365.4	1596.8	6.4
32.2	146.2	283.3	40.3	800.7	91.2	1213.7	437.4	1599.8	5.2
35.0	472.1	285.7	186.2	809.7	30.4	1217.7	286.4	1601.3	8.6
41.4	171.7	298.1	57.7	846.8	99.9	1240.1	327.5	1632.9	475.4
42.3	88.9	303.7	114.9	866.5	3.4	1254.3	28.9	1662.6	404.3
47.1	43.0	310.4	174.6	871.4	12.4	1255.0	507.6	1676.8	932.9
52.0	11.5	319.6	270.1	872.8	3.7	1256.6	717.8	1679.5	394.2
53.2	76.9	330.5	10.0	887.3	0.9	1259.3	193.1	1688.9	642.2
59.6	141.5	339.2	75.6	889.5	9.3	1259.9	468.0	1694.8	789.4
62.0	74.8	341.6	85.9	895.2	2.4	1265.9	151.1	1705.6	277.2
67.7	148.7	351.6	534.8	898.5	5.0	1267.6	634.9	1710.4	146.3
69.4	37.7	362.4	519.6	900.6	16.8	1278.2	210.9	1716.9	1291.3
72.0	98.8	367.4	502.0	905.9	12.7	1280.6	758.8	1717.8	929.1
74.9	77.6	371.6	17.6	927.4	36.1	1284.5	23.1	1734.1	266.3
77.4	97.1	373.6	124.0	940.6	31.4	1294.4	524.3	1743.8	951.0
79.8	15.9	396.1	107.7	954.4	2.0	1311.7	94.5	2956.2	53.5
80.9	349.5	412.3	129.0	960.1	15.6	1334.2	128.8	2962.0	37.1
85.1	77.5	417.2	57.5	963.2	95.8	1335.8	4.2	2964.3	85.2
85.5	83.8	423.0	133.0	965.0	171.9	1340.1	49.7	2965.1	50.9
88.6	211.9	434.2	42.6	968.1	19.5	1343.9	122.7	2965.7	56.8
91.5	27.4	435.3	47.7	968.5	101.5	1344.8	209.4	2966.1	96.3
92.5	16.4	444.0	67.0	974.9	63.0	1348.9	251.4	2969.3	41.8
99.5	23.8	451.4	10.0	976.7	10.3	1349.4	225.7	2977.1	20.9
101.3	176.9	464.7	15.9	978.8	12.8	1351.4	58.1	2978.5	31.9
103.0	37.6	470.4	38.4	983.4	67.1	1354.2	200.6	2978.8	25.2
103.8	122.5	487.2	145.7	987.3	49.1	1377.1	95.3	2979.6	22.3
106.9	129.8	491.9	391.4	994.4	2.3	1383.5	60.0	2985.7	27.0
109.8	24.7	506.2	146.6	996.0	14.0	1388.5	58.4	3006.7	9.4
115.1	40.7	514.3	377.7	1006.1	73.2	1390.4	53.5	3032.4	7.0
119.6	9.5	544.2	719.7	1013.2	48.9	1395.4	32.2	3036.3	8.3
126.7	88.8	550.9	29.8	1013.7	86.4	1397.2	76.0	3039.5	4.9
136.6	13.1	555.0	39.0	1014.9	20.8	1407.8	53.7	3042.9	6.2
144.4	35.6	567.8	81.8	1018.1	219.9	1407.8	38.4	3046.4	11.8
146.4	239.7	582.6	71.8	1057.3	27.2	1409.2	4.2	3051.3	6.4
153.4	37.8	585.5	50.4	1062.3	53.1	1409.5	111.9	3052.3	26.3
157.9	251.2	587.2	80.5	1073.2	35.8	1409.8	42.6	3056.7	13.0
159.4	3.8	590.3	38.1	1080.9	66.8	1410.1	19.0	3059.4	12.0
165.1	12.0	594.4	47.9	1083.9	35.2	1412.9	19.2	3060.1	11.5
168.5	53.1	606.9	234.8	1092.2	14.6	1416.9	89.9	3062.3	16.9
170.4	3.3	610.9	277.5	1124.0	7.5	1420.8	62.6	3081.7	12.9
175.8	29.8	646.2	8.5	1126.7	3.6	1422.2	31.0	3082.1	10.4
178.8	30.3	671.0	226.3	1127.8	1.4	1423.3	62.9	3082.7	13.4
179.9	24.8	677.1	66.4	1129.9	9.3	1423.9	34.3	3084.3	10.7
182.3	39.9	683.8	311.2	1132.4	2.1	1425.1	52.2	3085.0	12.7
183.6	119.1	690.0	39.7	1133.3	3.1	1426.7	14.5	3108.5	7.1
187.8	48.7	696.0	17.8	1134.3	3.1	1426.9	32.8	3113.0	5.8
188.2	42.0	701.1	113.7	1134.4	0.9	1427.5	17.2	3114.9	5.3
196.0	30.1	705.5	12.0	1136.9	4.2	1429.4	24.5	3119.7	12.8
200.1	132.9	709.6	93.4	1140.9	24.3	1430.4	11.3	3121.1	21.0
203.7	14.1	713.9	121.4	1162.7	15.6	1433.1	16.4	3123.7	26.2
208.5	30.1	726.4	57.6	1163.4	38.0	1433.3	75.5	3128.8	37.2
229.2	54.5	734.2	115.6	1164.9	1.8	1433.6	7.0	3287.1	853.6
238.0	44.9	739.6	20.7	1165.4	24.4	1434.0	33.0	3303.9	179.0
243.2	134.5	742.1	175.4	1166.7	20.3	1512.6	387.3	3324.4	557.5
246.4	115.5	744.9	174.4	1167.6	25.4	1520.8	86.8	3353.2	632.0
252.5	151.4	747.0	305.3	1188.1	184.2	1527.5	803.4	3388.8	536.8
254.2	91.4	755.5	131.0	1193.9	206.1	1530.6	504.4	3470.9	254.9

Table S12 Frequencies and dipole strengths of the infrared spectra of **BTA Gly^{Me}** [2,2,1,1-5/1] computed by the B3LYP-GD3BJ/cc-pVDZ method.

frequency cm ⁻¹	D 10 ⁻⁴⁰ esu ² cm ²	frequency cm ⁻¹	D 10 ⁻⁴⁰ esu ² cm ²	frequency cm ⁻¹	D 10 ⁻⁴⁰ esu ² cm ²	frequency cm ⁻¹	D 10 ⁻⁴⁰ esu ² cm ²	frequency cm ⁻¹	D 10 ⁻⁴⁰ esu ² cm ²
11.2	103.9	255.9	141.9	765.0	36.2	1198.1	122.6	1534.3	810.1
15.7	9.4	257.2	44.3	770.9	2.2	1202.8	314.7	1543.7	798.6
17.1	319.0	266.5	93.2	777.1	16.8	1206.2	1152.3	1594.3	18.8
26.3	62.9	269.3	107.0	780.6	25.1	1213.2	950.0	1596.6	59.1
29.5	170.9	280.9	26.2	796.4	82.1	1217.2	63.2	1600.8	35.8
31.0	112.7	286.7	343.7	809.5	7.8	1218.2	309.3	1601.8	3.0
38.2	138.4	299.8	79.2	841.8	134.0	1225.8	402.6	1640.8	457.0
40.8	16.4	302.9	49.9	866.6	31.1	1227.4	1246.8	1653.6	493.4
42.9	52.4	313.1	244.4	871.9	36.6	1240.1	277.4	1676.3	1043.1
44.9	98.3	318.7	7.3	873.6	1.2	1245.8	252.7	1682.7	583.4
51.3	125.8	324.8	241.5	881.6	17.1	1253.8	486.6	1694.9	851.0
53.3	109.8	334.6	105.0	884.9	4.1	1259.1	430.1	1706.9	180.6
58.8	130.4	342.7	525.5	891.0	4.3	1260.1	421.6	1709.9	443.7
60.3	109.8	345.4	430.8	899.8	13.7	1264.9	534.0	1714.8	566.7
62.1	109.3	350.9	59.6	902.9	14.5	1273.0	290.6	1717.0	964.5
65.5	59.7	357.1	372.1	927.3	43.8	1274.2	602.9	1720.0	771.1
71.5	101.1	364.0	363.7	930.6	18.0	1282.0	148.2	1748.8	465.3
73.7	33.2	370.0	221.2	936.7	1.4	1287.1	264.6	1761.7	696.5
76.7	49.7	392.1	76.7	947.9	50.1	1310.0	6.5	2956.3	59.2
77.1	87.8	398.1	76.1	960.2	15.8	1320.8	291.4	2957.5	55.8
81.0	118.6	418.6	115.9	961.2	16.4	1332.7	96.6	2962.1	20.6
84.0	48.2	425.1	111.1	965.5	127.5	1338.5	304.2	2964.1	35.8
84.5	121.9	436.8	18.5	966.6	25.0	1342.0	51.8	2966.2	75.4
86.9	16.9	441.9	63.9	972.6	105.9	1346.6	202.4	2966.4	49.8
93.3	38.0	450.0	58.7	974.3	48.4	1347.9	173.4	2967.8	67.2
100.0	34.3	464.6	42.9	975.4	143.0	1350.5	236.7	2968.1	24.1
101.3	184.6	469.8	97.7	987.9	1.0	1353.6	217.1	2976.7	21.2
105.9	65.6	477.2	40.3	990.3	31.6	1356.1	287.9	2977.9	26.3
108.1	103.5	494.5	115.7	993.3	34.1	1369.1	194.7	2978.2	36.1
109.9	135.7	503.7	325.7	994.7	29.1	1374.7	26.3	2978.9	46.1
115.4	178.3	509.9	274.4	997.9	84.3	1387.5	70.5	2995.6	3.4
120.1	17.2	528.7	254.0	1002.7	68.2	1388.5	69.1	3029.2	5.8
121.6	16.0	534.3	57.9	1007.6	31.0	1392.9	35.9	3031.3	27.1
124.6	57.7	543.1	60.6	1014.0	34.1	1399.2	78.8	3033.2	7.0
127.6	69.3	557.1	53.2	1017.2	80.3	1404.5	7.1	3035.2	6.7
135.2	107.9	562.8	174.8	1019.5	160.2	1406.2	16.9	3035.4	23.5
139.8	41.8	573.6	191.1	1063.2	31.4	1407.7	84.5	3037.2	4.2
143.1	216.9	577.8	272.1	1064.1	65.9	1408.9	23.9	3049.2	10.8
146.3	93.4	582.9	45.9	1072.3	41.5	1409.2	32.0	3055.1	12.4
150.6	121.5	586.0	56.4	1079.3	35.1	1410.9	28.5	3062.1	6.1
159.8	36.1	597.7	84.7	1085.0	28.0	1412.5	140.0	3062.5	12.9
163.1	109.0	605.1	488.3	1098.5	165.3	1413.7	138.3	3075.1	2.0
170.8	24.3	613.5	74.5	1124.0	7.3	1415.8	271.0	3076.1	18.8
172.7	118.2	638.3	231.9	1124.1	2.7	1417.8	101.9	3080.7	19.2
178.3	24.2	654.0	310.6	1127.9	3.1	1422.4	9.8	3083.2	9.8
178.5	245.7	656.6	25.1	1129.0	0.4	1423.5	2.9	3086.4	11.3
179.4	125.8	657.4	248.8	1129.4	22.3	1424.2	3.2	3086.7	9.6
180.8	23.5	678.2	326.8	1130.7	4.2	1424.5	17.4	3106.8	7.2
182.8	160.6	686.2	117.9	1132.8	3.7	1424.8	25.7	3117.6	6.9
189.7	65.0	691.7	51.3	1134.2	1.0	1425.1	78.9	3125.9	4.4
190.6	30.1	697.0	110.4	1142.9	14.9	1426.7	18.2	3129.8	15.8
197.3	30.0	699.0	70.6	1144.7	19.4	1427.3	12.3	3132.1	36.4
199.8	90.6	708.5	56.8	1159.7	27.9	1428.4	15.7	3133.0	13.2
206.7	4.7	716.5	105.1	1162.5	12.5	1430.4	17.9	3136.1	6.3
212.1	44.6	730.1	122.3	1163.3	10.0	1431.4	18.2	3308.2	600.3
224.0	91.9	735.0	38.0	1163.9	17.5	1433.4	14.5	3338.7	344.5
233.8	30.1	736.8	206.9	1167.6	22.0	1501.0	645.5	3347.1	633.3
242.3	63.8	741.7	281.2	1170.5	6.2	1518.5	278.0	3419.2	222.6
249.5	149.2	741.8	95.0	1188.1	341.0	1525.0	93.7	3448.6	341.6
252.6	33.0	750.8	98.0	1197.3	10.3	1533.1	1038.7	3468.1	132.3

Table S13 Frequencies and dipole strengths of the infrared spectra of **BTA Gly^{Me}** [1,1,1,1,1,1-6/0] computed by the B3LYP-GD3BJ/cc-pVDZ method.

frequency cm ⁻¹	D 10 ⁻⁴⁰ esu ² cm ²	frequency cm ⁻¹	D 10 ⁻⁴⁰ esu ² cm ²	frequency cm ⁻¹	D 10 ⁻⁴⁰ esu ² cm ²	frequency cm ⁻¹	D 10 ⁻⁴⁰ esu ² cm ²	frequency cm ⁻¹	D 10 ⁻⁴⁰ esu ² cm ²
21.2	6.5	279.9	12.9	777.9	14.9	1207.1	1244.7	1529.8	1969.2
21.3	11.9	280.5	52.8	778.1	14.9	1207.2	1295.4	1538.6	0.5
25.9	87.1	280.7	57.8	785.0	5.6	1207.5	59.1	1600.4	4.2
26.6	104.3	286.9	0.4	785.3	5.6	1210.9	250.4	1600.5	3.3
29.3	2258.1	287.1	0.1	788.5	53.8	1211.0	230.9	1601.4	3.3
29.8	58.4	290.7	0.0	799.5	0.0	1214.0	0.5	1601.5	2.2
48.7	55.5	309.9	465.1	867.2	15.5	1257.6	110.9	1659.8	25.3
48.8	65.6	310.1	466.4	867.3	15.7	1257.7	142.9	1670.1	898.9
50.8	3.2	314.4	128.5	870.8	3.1	1259.1	80.1	1670.1	882.3
55.7	0.4	314.7	123.0	870.9	3.2	1259.5	1145.6	1673.0	1.2
56.1	0.4	333.5	0.2	893.3	0.0	1259.6	1181.1	1679.0	771.2
62.4	0.9	334.6	0.0	895.6	4.7	1260.8	4.0	1679.0	769.0
66.8	243.2	368.1	670.6	895.9	8.8	1265.3	0.2	1709.0	9.1
66.9	225.9	368.2	669.1	896.0	9.0	1266.9	430.5	1709.1	8.5
71.4	8.2	372.8	28.3	899.4	15.3	1284.0	1.8	1711.7	0.2
71.9	8.4	372.8	32.4	899.5	15.6	1284.2	2.4	1716.5	1544.1
77.2	1.0	374.4	0.3	956.8	31.8	1289.6	609.1	1716.5	1544.1
81.2	187.9	377.4	39.9	957.9	0.2	1289.8	609.9	1717.0	950.1
81.5	181.2	411.5	42.2	963.8	330.6	1334.2	5.2	2965.3	29.6
85.1	24.5	411.6	33.7	964.2	90.5	1335.6	0.1	2965.3	42.2
85.6	17.0	414.1	228.2	964.2	94.9	1342.6	62.7	2965.4	53.2
89.6	157.6	414.1	237.2	966.1	0.3	1346.8	135.7	2965.8	163.9
92.4	1.8	421.1	27.7	967.7	30.9	1346.9	124.0	2966.0	172.2
95.4	237.0	421.7	0.6	967.7	34.0	1347.8	1.0	2966.2	13.7
95.8	222.5	458.7	76.2	971.6	2.6	1348.7	426.1	2982.3	10.0
97.3	16.3	459.0	77.0	972.5	2.9	1348.8	412.6	2982.5	5.1
97.8	2.5	463.2	1.6	972.9	1.6	1349.5	159.6	2982.6	3.9
102.3	215.9	464.0	0.6	974.1	1.9	1352.5	0.3	2982.6	63.4
102.4	181.6	489.1	65.1	988.0	4.0	1386.9	43.4	2982.8	69.8
103.6	73.3	489.2	73.8	988.1	86.8	1387.0	43.5	2982.9	13.4
104.1	76.0	493.3	383.9	995.6	29.5	1387.6	86.0	3043.6	12.2
106.1	1.0	493.5	383.3	996.5	0.1	1391.1	74.9	3043.9	14.6
118.4	30.4	542.8	1194.9	1014.0	79.1	1391.2	76.7	3044.2	15.2
118.6	32.1	561.6	0.2	1014.1	80.0	1392.1	0.0	3044.2	3.6
123.3	591.7	572.9	312.2	1015.8	0.5	1407.6	39.5	3044.3	1.2
144.5	0.0	578.4	15.3	1016.0	0.8	1407.6	49.4	3044.5	0.5
150.4	29.9	579.1	15.8	1056.0	0.5	1407.7	52.6	3060.9	4.6
151.6	39.3	591.2	127.4	1056.2	64.6	1409.3	58.5	3060.9	7.9
152.2	37.8	591.3	128.7	1078.4	26.8	1409.4	60.8	3061.0	17.4
154.7	0.3	595.2	0.1	1078.4	24.8	1409.5	3.2	3061.7	22.6
156.7	7.0	598.3	310.7	1079.3	90.8	1422.3	53.3	3061.8	19.8
157.3	4.6	601.9	33.4	1079.3	92.6	1422.6	64.7	3061.9	18.0
172.5	11.1	602.6	36.9	1131.4	0.2	1423.2	96.4	3083.4	5.5
172.9	0.7	625.7	0.1	1131.4	0.0	1423.5	40.7	3083.5	0.3
179.1	57.4	665.6	186.0	1132.4	3.0	1423.9	31.5	3083.5	26.6
180.0	74.3	666.6	185.4	1132.6	3.0	1424.4	19.0	3083.5	0.3
183.0	57.0	679.3	312.3	1134.0	2.1	1428.2	14.8	3083.7	17.0
183.8	67.7	697.6	0.2	1134.1	1.5	1428.3	12.1	3084.0	13.0
188.6	0.1	701.2	116.4	1134.6	1.1	1428.6	15.5	3119.3	2.5
189.6	2.3	701.2	119.7	1134.7	4.2	1428.8	6.1	3119.8	2.4
193.4	3.3	704.6	2.2	1134.9	3.3	1433.2	5.5	3119.9	10.8
193.6	4.5	704.6	3.5	1135.4	3.8	1433.3	13.6	3120.0	22.4
199.3	3.3	724.6	95.3	1166.0	0.7	1433.4	33.9	3120.1	54.1
199.8	3.9	731.0	0.0	1166.2	13.5	1434.0	45.8	3120.6	33.2
240.3	157.2	742.6	1.3	1166.2	16.8	1434.1	42.8	3340.7	59.4
240.8	164.5	742.6	1.2	1166.4	34.7	1434.2	34.2	3340.9	131.5
248.5	4.5	745.5	56.7	1166.9	29.0	1518.9	32.8	3341.3	118.0
249.0	253.2	745.6	56.1	1167.0	34.8	1519.3	29.1	3351.2	106.3
249.3	253.7	746.8	68.7	1191.5	109.2	1527.8	130.6	3354.9	1417.5
254.9	16.8	747.1	638.6	1193.7	0.1	1529.6	1969.0	3355.3	1399.8

Table S14 Frequencies and dipole strengths of the infrared spectra of **BTA Gly^{Me}** monomer computed by the B3LYP-GD3BJ/cc-pVDZ method.

frequency cm ⁻¹	D 10 ⁻⁴⁰ esu ² cm ²	frequency cm ⁻¹	D 10 ⁻⁴⁰ esu ² cm ²	frequency cm ⁻¹	D 10 ⁻⁴⁰ esu ² cm ²	frequency cm ⁻¹	D 10 ⁻⁴⁰ esu ² cm ²	frequency cm ⁻¹	D 10 ⁻⁴⁰ esu ² cm ²
6,9	402,2	875,2	33,8	1688,6	82,0				
9,3	33,3	875,2	33,7	1696,3	781,6				
9,5	31,9	910,7	17,0	1696,3	781,1				
32,4	61,6	936,7	22,4	1757,9	482,2				
32,4	60,4	945,1	12,6	1757,9	478,2				
34,4	14,4	945,3	13,2	1758,0	79,8				
37,2	4,0	953,3	33,6	2941,4	72,7				
37,5	3,0	953,4	34,5	2941,4	71,8				
44,2	316,0	976,6	5,9	2941,6	5,7				
58,6	377,1	984,5	22,6	2960,5	47,1				
58,9	25,7	984,7	22,2	2960,5	48,0				
59,0	21,9	987,1	66,5	2960,6	22,8				
98,3	272,0	988,9	144,6	2974,5	7,7				
98,5	72,9	988,9	144,9	2974,7	8,4				
98,5	94,6	991,7	14,4	2974,8	9,4				
122,7	12,1	1091,8	9,3	3040,0	16,7				
122,7	31,5	1092,4	219,0	3040,0	16,2				
122,8	37,6	1092,5	218,0	3040,0	30,7				
147,4	202,9	1125,0	3,0	3078,3	18,4				
147,6	199,8	1125,1	2,9	3078,3	17,2				
155,9	90,8	1125,1	3,1	3078,3	12,6				
162,7	112,8	1134,5	30,9	3109,8	0,7				
162,7	115,0	1134,5	30,9	3110,1	9,1				
171,0	344,8	1159,2	52,3	3110,2	9,2				
183,4	254,3	1159,2	51,6	3474,2	44,4				
208,5	33,1	1159,3	9,9	3474,3	101,7				
208,6	33,1	1174,8	2,0	3474,4	101,7				
236,9	40,1	1178,7	15,6						
236,9	40,6	1178,8	15,4						
239,2	8,6	1185,1	8,4						
257,9	399,9	1194,0	1648,6						
257,9	398,9	1194,1	1654,0						
314,9	10,8	1205,9	200,0						
330,8	39,9	1234,8	376,8						
341,0	496,4	1234,9	373,4						
341,0	497,0	1237,9	3,5						
413,0	118,4	1282,0	122,9						
413,0	118,4	1339,9	1357,9						
431,0	238,0	1339,9	1358,3						
454,8	46,3	1340,8	7,3						
455,1	46,7	1356,0	79,2						
494,2	520,7	1408,5	23,3						
502,5	96,3	1408,6	23,7						
502,8	95,8	1408,6	30,6						
539,5	242,0	1411,0	327,8						
539,7	242,9	1411,0	326,4						
564,8	189,0	1412,1	77,1						
566,0	72,7	1416,3	67,1						
566,1	73,7	1416,4	67,5						
582,9	57,1	1421,8	0,4						
655,0	141,3	1424,3	35,7						
655,1	140,9	1424,4	35,6						
664,0	31,6	1427,0	3,2						
669,2	1,0	1427,9	0,4						
731,0	220,9	1427,9	0,4						
732,1	135,9	1493,0	1671,9						
732,1	136,0	1493,0	1671,4						
765,4	1,2	1503,3	47,0						
765,4	1,1	1598,2	6,4						
824,0	8,0	1598,2	6,4						

References

1. B. Gong, C. Zheng and Y. Yan, *J. Chem. Cryst.*, 1999, **29**, 649-652.
2. A. D. Lynes, C. S. Hawes, K. Byrne, W. Schmitt and T. Gunnlaugsson, *Dalton Trans.*, 2018, **47**, 5259-5268.
3. S. Hoyas, V. Lemaur, Q. Duez, F. Saintmont, E. Halin, J. De Winter, P. Gerbaux and J. Cornil, *Adv. Theory Simul.*, 2018, **1**, 1800089.
4. L. Calabi, A. Maiocchi, M. Lolli and F. Rebasti Diagnostic imaging contrast agent with improved in-serum relaxivity WO9805625, 1998.